



# Evaporative Moisture Sources of Colorado's Front Range: A Case Study of the Exceptionally Wet May-July Season of 2023

Katherine V. Humphreys<sup>1</sup>, Patrick W. Keys<sup>2</sup>, Russ S. Schumacher<sup>1,3</sup>, Jacob Escobedo<sup>1</sup>, Peter Goble<sup>3</sup>,

<sup>1</sup>Department of Atmospheric Science, Colorado State University, Fort Collins, Colorado, USA

5 <sup>2</sup>Department of Earth and Environment, Boston University, Boston, Massachusetts, USA

<sup>3</sup>Colorado Climate Center, Colorado State University, Fort Collins, Colorado, USA

*Correspondence to:* Katherine V. Humphreys (kathum.earth@gmail.com)

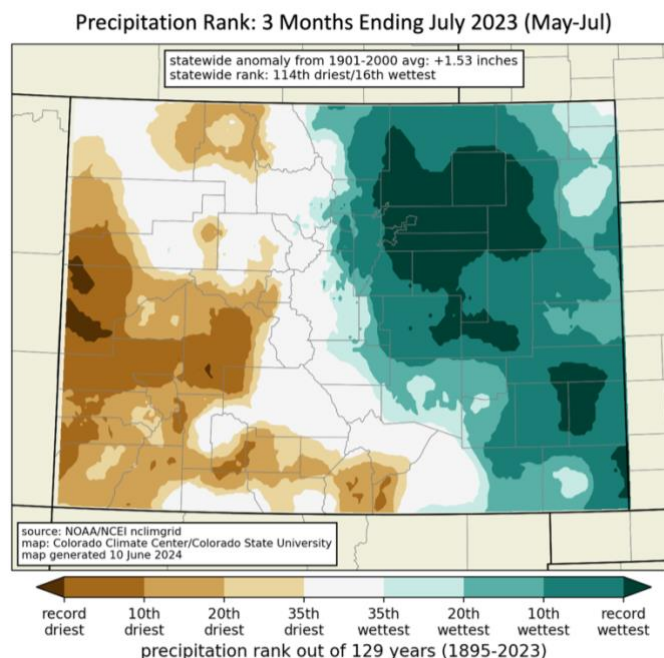
**Abstract.** In 2023, parts of eastern Colorado experienced their wettest three-month period (May - July) out of 129 years of record. This extreme precipitation led to flash flooding, road washouts, and significant property damage among Colorado communities along the Front Range including Denver, Boulder, and Fort Collins. Although the Front Range is the most populated region in Colorado, few studies have explored the evaporative origin of Front Range precipitation. To better anticipate and understand extreme precipitation events across the region, we focus our investigation on the evaporative origin of the extreme precipitation in May, June, and July (MJJ) of 2023 and how it compares to moisture sources during the previous two decades. This study uses the Water Accounting Model 2 Layers (WAM2layers) and hourly ERA5 reanalyses to quantify the evaporative sources of precipitation in Colorado's Front Range during MJJ of 2023 and over the past 23 years (2000-2022). Our moisture source analysis reveals that for the Front Range region in May-July of 2023: (1) the three primary moisture sources are the Pacific Ocean, the western United States, and Colorado itself, contributing just over 66.2% of total precipitation; (2) historically, those same regions dominate evaporative contributions in MJJ, but terrestrial contributions and local moisture recycling (i.e., precipitation that recently evaporated from within the Front Range) in May-July of 2023 accounted for a slightly greater proportion of precipitation than on average; (3) moisture sources in May-July 2023 were a statistical outlier in terms of the magnitude of moisture contributed to the Front Range; and (4) anomalous evaporative contributions in May-July 2023 originated from a broad range of regions, more consistent with the leading mode of moisture source variability, which reflects widespread anomalies from Colorado and the Pacific Ocean, rather than the second leading mode characterized by a north-south dipole in anomalous contributions from regions north and south of the Front Range. This research provides new insights into the origins of extreme rainfall in the summer of 2023 as well as the historical moisture sources of warm-season precipitation in the Front Range.

## 1 Introduction

In May through July of 2023, parts of eastern Colorado experienced its wettest three-month period out of 129 years of record (Colorado Climate Center, 2024; Fig. 1). Multiple heavy and convective rain events during these three months caused some regions across eastern Colorado to receive over 400 mm of rain, exceeding their average annual precipitation. Out of



Colorado’s 5.7 million residents, the Front Range urban corridor is home to an estimated 4.9 million people (U.S. Census Bureau, 2020), making this region particularly susceptible to increased damage from heavy rainfall events. This record-breaking rainfall affected many residents along the Front Range in the form of urban flooding, property damage, and infrastructure damage such as road washouts and sinkholes.



35

**Figure 1: Ranking of precipitation from May-July 2023, compared to all 129 May-July periods in the NOAA’s Monthly U.S. Climate Gridded Dataset (NClmGrid) precipitation dataset. The areas in darkest green had record-breaking wet conditions in 2023. Figure adapted from the Colorado Climate Center’s Climate at a Glance webpage (Colorado Climate Center, 2024).**

### 1.1 Moisture Source Research

40 One useful lens to study precipitation is through its evaporative source regions or evaluating where that moisture last evaporated from before falling as precipitation. Studying moisture sources provides insight into how water is exchanged between the surface and the atmosphere, and overall, furthers our knowledge of the hydrologic cycle (Gimeno et al., 2020). Brubaker et al. (2001) suggests that proper identification of precipitation source regions could improve seasonal to interannual precipitation forecasting. Koster et al. (2004) found that contributions from local, terrestrial moisture sources could be  
45 important to precipitation anomalies in eastern Colorado due to a coupling between soil moisture and precipitation in the region. Through the exploration of Front Range moisture sources, this study aims to better understand the extremely wet 2023 May-July season and identify specific regions that could lead to better anticipation of extreme wet seasons in the future.



50 There is an extensive and growing body of research exploring extreme precipitation through the identification of its moisture sources and the associated pathways of water vapor transport. The specific moisture sources and mechanisms behind water vapor transport can vary considerably by location (Gimeno et al., 2020), so many researchers have opted to conduct regional analyses of precipitation at multiple timescales (i.e. multi month to sub weekly periods). Previous studies have explored the moisture sources of regions within Europe (e.g. Gustafson et al., 2010; Pinto et al. 2013; Rios-Entenza and Miguez-Macho, 55 2014; Ciric et al., 2018; Cloux et al., 2021), Asia (e.g. Zhao et al., 2016; Liu et al., 2021; Zhang et al., 2023; Liu et al., 2024; Zhang et al., 2024), Africa (e.g. Durmond et al., 2011; Rapolaki et al., 2021), and South America (e.g. Arias et al., 2015; Marengo et al., 2013). There is also abundant research studying the origins of precipitation in United States, including regions such as the Southwestern US (e.g. Jana et al., 2018; Erlingis et al., 2019a; Erlingis et al., 2019b; Skinner et al., 2023), Midwestern US (e.g. Dirmeyer and Brubaker, 1999; Yang et al., 2023; Kim and Dominguez, 2023), and broadly across the 60 country (e.g. Dirmeyer et al., 2009; Hu and Dominguez, 2015).

Previous literature has identified moisture sources of eastern Colorado during wet or extremely wet periods. However, the few studies conducted in this region are either outdated or span too large of a region to study the precipitation events during May-July of 2023. Eden et al. (2016) found that for the September 2013 Colorado flood event, eastern Colorado moisture sources were substantially different from September climatological sources. Jana et al. (2018) used a particle tracking model 65 (HYSPLIT) to explore the moisture sources of warm season rainfall (July-September) in Eastonville, Colorado from 1979 to 2013. However, these previous studies only analyze July-September moisture sources up until 2013, making it unsuitable for diagnosing the evaporative origins of precipitation after or during May and June. Erlingis et al (2019b) identified the Gulf of Mexico, Gulf of California, and Southwestern US as moisture sources of flash flooding events in Colorado and New Mexico. Skinner et al. (2023) found that during the wettest springs and summers in the Southwestern US, anomalous precipitation 70 predominantly originated from remote sources, and moisture recycling within the region amplified these already wet seasons by up to 30%. Both investigations utilize study regions spanning multiple states and include precipitation not only from Colorado's Front range but also including rainfall from New Mexico and Arizona. Local features such as topography, land cover, and circulation patterns inherently shape water vapor transport and availability in the atmosphere (Brubaker et al., 2001; van der Ent et al., 2010; Gimeno et al., 2020). Thus, highlighting the need for updated, regional analyses to adequately capture 75 the evaporative origins of precipitation in Colorado's Front Range.

## 1.2 Study Goals

Our goal is to better understand the extreme precipitation in the May-July season of 2023 by quantifying where it last evaporated from and putting those results into the context of the past two decades (2000-2022). Exploring this region's historical sources of precipitation provides a baseline in which we can compare 2023 moisture sources to. If the dominant 80 moisture sources in May-July of 2023 were substantially different than average, then we could potentially identify source regions that are important to extreme precipitation in the Front Range. In doing so, we would be building some capacity to better anticipate or foresee extremely wet seasons before they occur. Ultimately these goals were designed to inform the



emergency management team within the Colorado Water Conservation Board (which partially funded this project) by providing a better understanding on how the extreme precipitation in the May-July season of 2023 unfolded. Furthermore, providing twenty-four years of continuous moisture source data for the Front Range, the most populated region in Colorado, provides a foundation to understand the long-term moisture transport into the region. Although this paper focuses on Colorado's Front Range, we analyzed four other regions within eastern Colorado that also experienced an extremely wet May-July season in 2023. These results can be found in the Appendix B.

## 2 Methodology

### 2.1 Water Vapor Tracking Methods

Water vapor in a given area can be thought of as the sum of two components: (1) moisture that evaporated remotely and advected into a region and (2) moisture that evaporated from within the region itself (Burde and Zangvil, 2001). Moisture that evaporates from the land surface and returns as precipitation within the same region is a process called moisture recycling (Brubaker et al., 1993; Keys et al., 2012; Kostner et al., 2004; Skinner et al., 2023). To quantify the source regions of precipitation, it is essential to have a method for tracking water vapor as it moves through the atmosphere. Observational data related to moisture sources typically rely on measuring stable isotopes of water to infer the origins of precipitation in the region (Dansgaard, 1964; Gimeno et al., 2020; Sprenger et al., 2016). To address the goals of our study, these observational approaches are too spatially and temporally limited for a multi-year moisture source analysis in eastern Colorado. Furthermore, isotope analysis cannot provide the level of spatial detail needed to conclude what specific geographical source regions are important to Front Range precipitation intended for this analysis (van der Ent et al., 2013). Current methods of calculating the evaporative sources of precipitation mostly rely on model-based tools that use numerical tracking methods (Gimeno et al., 2020; Insua-Costa and Miguez-Macho, 2018). The types of numerical tracking methods can generally be defined by two characteristics: (1) whether the methods are online or offline and (2) whether they use a Lagrangian or Eulerian framework (van der Ent et al., 2013; Insua-Costa and Miguez-Macho, 2018).

In online methods, water vapor tracking occurs concurrently as the weather or climate model progresses in time and simulates various atmospheric phenomenon (e.g. Bosilovich and Schubert 2002; Knoche and Kunstmann, 2013; Rios-Entenza and Miguez-Macho, 2014). Offline methods use meteorological variables after reanalysis becomes available or after the climate/weather model has completed to then calculate the evaporative origins of rainfall independently (e.g., Tuinenburg et al., 2012; Tuinenburg and Staal, 2020). One of the major discrepancies in using either online or offline approaches is the computational time needed to run these methods, with online approaches typically being more computationally expensive. Eulerian approaches track the budget of moisture that enters and exits a given column of atmosphere with a fixed grid system (e.g., van der Ent et al., 2010). Lagrangian approaches track the pathway of moisture through time following specific parcels of air as they travel across the globe (e.g., Wei et al., 2013). This current work uses an Offline, Eulerian approach due to their inexpensive computational nature compared to online, Lagrangian techniques.



## 115 **2.2 Model: WAM2layers**

To estimate the moisture for Colorado's Front Range, we used the WAM2layers model (Water Accounting Model 2-Layers, v3.0.0-beta.5). This specific version of the WAM2layers model used in this study can be downloaded from van der Ent et al. (2023), and more detailed information about version 3 can be found within Kalverla et al. (2025). Previous versions of the WAM2layers model are documented in van der Ent et al. (2010) and van der Ent et al. (2014). This section will first describe  
120 the model in general, how it was specifically used in this study, model assumptions, and close with other scholars who have used this model before.

The WAM2layers model is an Offline, Eulerian model used to track water vapor forward and backward in time based on the conservation of atmospheric moisture, sometimes referred to as water balance (van der Ent et al., 2014). Instead of simulating atmospheric processes like a general circulation model, the WAM2layers model acts as an accounting system that tracks the  
125 exchange of water vapor between grid cells using input meteorological data, most often a reanalysis dataset (Kalverla et al., 2025). Atmospheric moisture balance implies that the change in water vapor overtime must be equal to the horizontal and vertical fluxes in and out of the grid cell as well as the land-atmosphere moisture exchanges via evaporation and precipitation (van der Ent et al., 2014). Some important limitations of this model include the exclusion of liquid and solid water in water balance calculations (although adjusted for ad hoc inside the model), inability to explicitly resolve vertical exchanges of  
130 moisture between the upper and lower layers (vertical moisture transport is treated as a balance closure term), and the reduction of the atmosphere to two layers. Further information about the WAM2layers model can be found in van der Ent et al (2014) and Kalverla et al (2025).

In this study, we only utilized the backward tracking mode of the WAM2layers model, commonly referred to as backtracking, to identify where Front Range precipitation last evaporated from. The backtracking process begins with inputs of global hourly  
135 meteorological data and a defined region of interest. Then, the tracking progresses backward through time, accounting for water vapor that fell as precipitation within the region to where it most recently evaporated from. This process is then repeated over the indicated period. Output from backtracking consists of daily tracked evaporation data on a latitude longitude grid according to the resolution of the input meteorological data. Tracked evaporation is defined as the component of a given grid cell's total evaporation that will later fall as precipitation in the given region of interest (i.e. Colorado's Front Range defined  
140 in Sect. 2.4). For our purposes, we decided to aggregate daily tracked evaporation to the monthly scale for further confidence in our results at the monthly scale instead of the daily timeframe.

We backtracked Front Range precipitation from 19 December 2023 to 1 January 2000. However, in our analysis, we do not include data from December, November, October, nor September of 2023 to allow more than three months of spin-up time for the model. Since water vapor is estimated to have a short lifetime in the atmosphere of around nine days on average (van der  
145 Ent et al., 2014; van der Ent and Tuinenburg, 2017), three months is ample time required for the WAM2layers model to reach a stable state. We also decided to run the WAM2layers model with a limited domain of only the Northern Hemisphere from 80°N to 0°N/S to reduce the amount of core hours needed to run the model and store output. Limiting the domain to below



80°N latitude is a common practice when using the WAM2layers model because at high latitudes, the model's method for moving moisture between grid cells can lead to unrealistic distribution of water vapor, a known issue related to numerical diffusion (Kalverla et al., 2025). To ensure our results are unchanged by a reduction in model domain, we conducted a sensitivity analysis where we compared a global domain run to the abbreviated domain used in this study. Results can be found in the appendix, but in brief, reducing the domain to exclude the Southern Hemisphere did not dramatically affect the results of this study but did, however, dramatically reduce the computational time of the model (Figure A6 in the appendix).

The results of this study are all derived from the WAM2layer model's tracked evaporation variable. Later in this paper, we discuss the average evaporative contribution of varying regions to Front Range precipitation. For clarity, we provide a description of how those values were calculated. Beginning with monthly tracked evaporation data produced by the WAM2layers model, we select the targeted month or months and take their mean through time. This produces a map of average grid cell evaporative contribution to the Front Range during the selected period (e.g. May or May-July). We then multiply this map by a binary mask of each source region with 1 representing a grid cell inside the region and 0 indicating outside of the source region. For reference, a map showing each source region in this study can be found in the appendix. Finally, we take the spatial sum of all grid cells to determine the evaporative contributions of the specified source region. To be clear, the average regional contribution is not the simple average of regional contribution over time. We calculated regional contributions in this way such that their relative contributions would all add up to 100% and be directly comparable to regional contributions in the May-July 2023 season.

### 2.3 Data

The WAM2layers relies on meteorological variables from the 0.25-degree latitude-longitude ERA5 Reanalysis dataset produced by the European Centre for Medium-Range Weather Forecasts (Hersbach et al., 2020). For this project, we use variables analyzed hourly that include specific humidity, zonal and meridional wind speed, surface pressure, evaporation, and precipitation. In addition to the meteorological variables from ERA5, we also used ECMWF's land-sea mask to quantify the evaporative contributions of terrestrial versus aquatic regions. This land-sea mask assigns each cell a value ranging from 0 to 1 representing the cell's land to water ratio based on land surface calculations last updated in December of 2019. ERA5 is the most current version of ECMWF's global climate reanalysis data product and performs well against precipitation observations in North America (Crossett et al., 2020; Beck et al., 2019; Tarek et al., 2020). Since the Front Range region sits just east of the Rocky Mountains, local details of precipitation are unable to be well represented.

Since ERA5 precipitation datasets do not directly assimilate in-situ precipitation observations into its precipitation product and is known to have trouble representing convective precipitation (Hersbach et al., 2020), a full comparison of ERA5 precipitation to the Parameter-elevation Regressions on Independent Slopes Model (PRISM) monthly precipitation totals is included in Appendix section A.1. The PRISM monthly precipitation dataset was a natural choice for comparison due to its gridded nature, incorporation of in-situ precipitation observations, and ability to resolve complex terrains (Daly et al., 2021). We find that although there are substantial differences in the amount and spatial distribution of precipitation in eastern Colorado, ERA5 can



correctly capture May-July of 2023 as very anomalously wet season compared to average, making it well suited for the purposes of our analysis.

## 2.4 Study Region: Colorado's Front Range

This study uses the Front Range region (FTR) of the alternate climate divisions specifically developed for Colorado by Schumacher et al. (2024). The FTR region contains major cities such as Denver, Fort Collins, Greeley, Aurora, and Boulder. To be clear, these alternate climate divisions are not NOAA's (National Oceanic and Atmospheric Administration) official climate divisions, which characterize Colorado regions by river basin. Instead, these alternate climate divisions characterize regions in Colorado by climate variability (Schumacher et al., 2024). For our specific purposes, we focus on the Front Range region of Colorado's alternate climate divisions since this region both experienced extreme precipitation in May-July of 2023 and is the most populous region among all 11 alternate climate divisions. We adapted the original FTR definition from Schumacher et al. (2024) to a quarter degree by quarter degree grid as depicted in Figure 2, and this region contains major cities such as Denver, Fort Collins, Greeley, Aurora, and Boulder. We note that we also analyze four other alternate climate divisions in eastern Colorado (the eastern Plains region, High Mountain Valley region, Pikes Peak region, and the Arkansas Basin region) that also experienced an extremely wet May-July season in 2023. Results for these regions can be found in Appendix B.

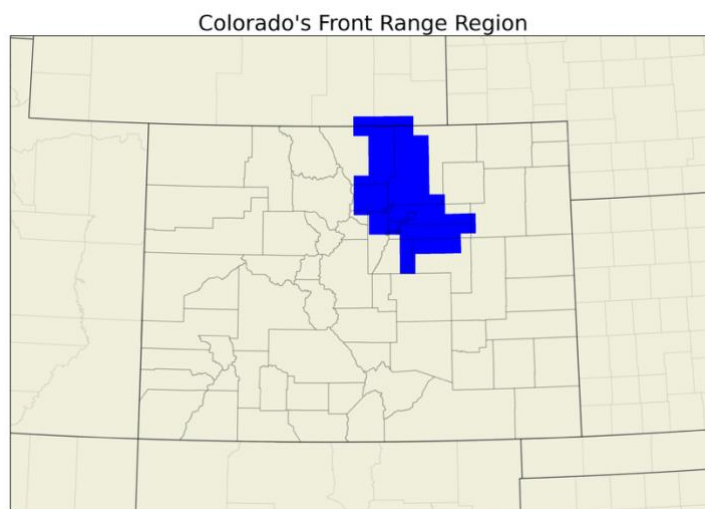


**Figure 2: Map of Colorado depicting the Front Range region in blue. Dark grey lines represent state boundaries, and the lighter grey lines represent county boundaries.**

## 2.5 K-Means Clustering Analysis

To identify how moisture sources in May-July of 2023 compared to individual years instead of a climatological average, we applied a k-means clustering analysis to tracked-evaporation anomalies accumulated across May-July (MJJ) from 2000 to 2023. This method is an unsupervised machine learning algorithm chosen for its ease of physical interpretation and minimal



required user inputs, reducing the interference from researcher specific bias. The goal of k-means clustering is to minimize the distance between each sample and the centroid of its assigned cluster and maximize the distance between the sample and  
205 centroids of different clusters (Lloyd, 1982). For the purposes of this study, this method will group all twenty-four May-July seasons (2000-2023) such that seasons with the most similar moisture source anomaly patterns will be sorted into the same group and that each cluster will be as distinct from each other as possible. This allows us to understand which individual MJJs are most similar to the 2023 MJJ season, further putting this extreme season into context.

To do so, we used Scikit-Learn's k-means clustering algorithm as described in Pedregosa et al. (2012). In deciding how to  
210 specify "k", i.e. the number of clusters to create, we used clustering metrics in combination with our personal knowledge of moisture sources to assess the optimal number of clusters and avoid over-fitting. Since there are only twenty-four MJJ periods between 2000 and 2023, we decided to limit the maximum number of clusters to ten to avoid over-fitting. Using more than ten clusters would decrease the interpretability of the results and could inhibit our ability to contextualize moisture sources in MJJ of 2023. The further selection of our k value relies on a clustering metric, the elbow method. Results of the elbow method are  
215 described in Sect. 3.3. To ensure cluster stability, the results shown in Sect. 3.3 are after 10,000 iterations.

## 2.6 Empirical Orthogonal Function (EOF) Analysis

Empirical orthogonal function (EOF) analyses, sometimes referred to as principal component analysis (PCA), is a popular and robust method among the climate research community to study spatial patterns of the major modes of variability for a given variable. In previous moisture source research, they have been applied to identify the spatial patterns of major modes of  
220 moisture source variability for a specific study region (e.g. Keys et al., 2014; Hu and Dominguez, 2015). In this study, we use tracked evaporation anomalies from the WAM2layers model to explore the interannual patterns of moisture sources associated with Front Range precipitation. Specifically, we analyzed tracked evaporation anomalies across May-July from 2000 to 2023 by removing the grid cell mean with respect to time. Due to memory constraints, we reduced the size of the tracked evaporation data by only including cells within the contiguous US and some of the surrounding oceans (67.0° W to 134.0° W longitude  
225 and 23.0° N to 49° N latitude). Our results are thus constrained to the portion of Front Range moisture sources that are located within these bounds. Our goal was to analyze how moisture sources across the 2023 MJJ season relate spatially to the major patterns of moisture source variability of Front Range precipitation. Essentially identifying which mode of variability was most important to moisture source anomalies in MJJ of 2023.

## 3 Results

230 The results of our study are organized into four subsections as follows: (1) moisture sources associated with the 2023 May-July season, (2) comparison to average MJJ moisture source from 2000 to 2022, (3) comparison to individual MJJ season moisture sources through k-means clustering, and (4) contextualization of 2023 MJJ moisture sources through an EOF analysis.

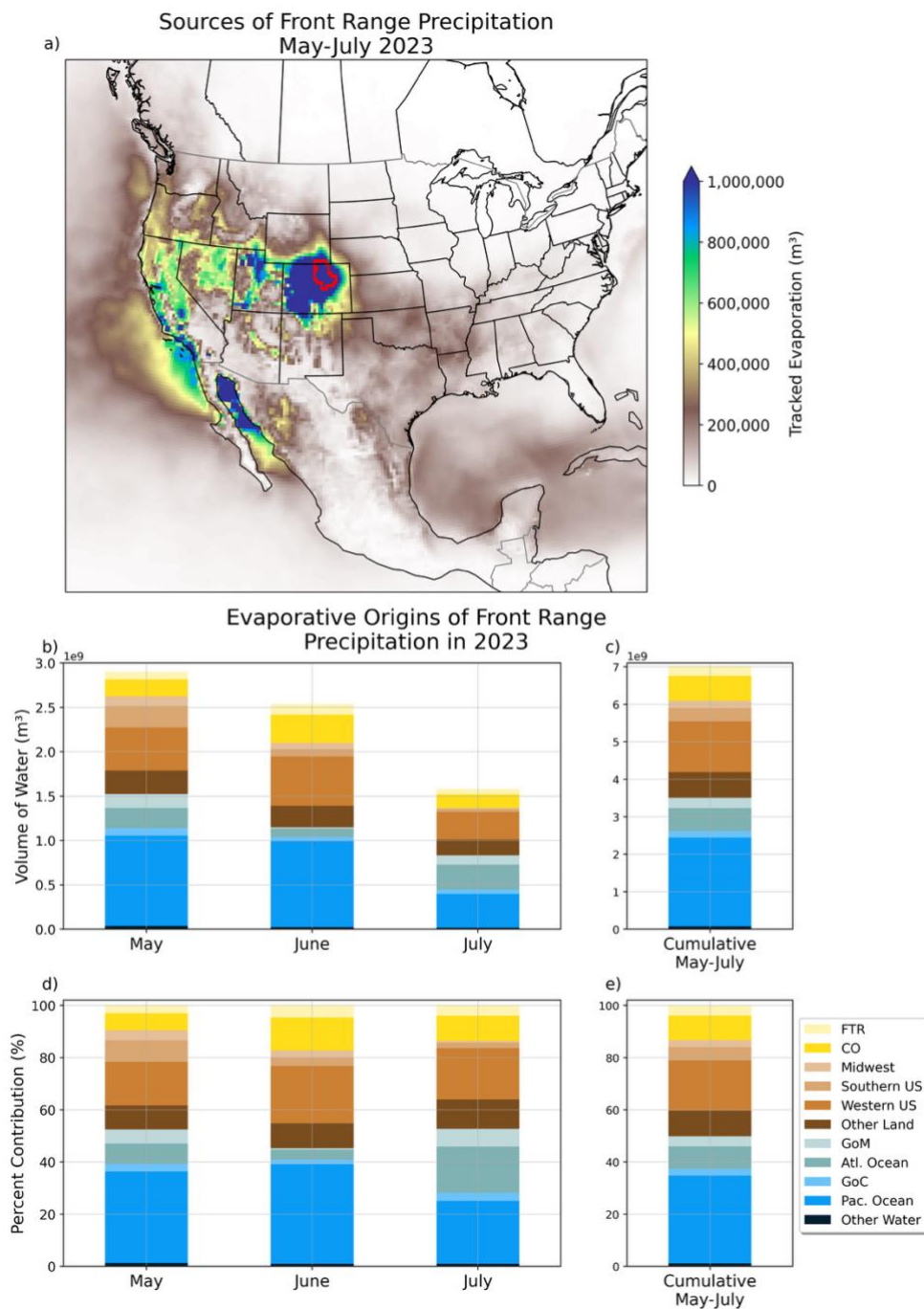


### 3.1 Moisture Sources of May, June, and July 2023 Precipitation

Here we discuss the moisture sources of Front Range precipitation in the months of May, June, and July of 2023 spatially (Fig. 235 3.a), by absolute regional contribution (3.b and 3.c.), and by regional contributions relative to total precipitation (3.d and 3.e). Bar chart colors indicate the different evaporative source regions: terrestrial sources are shown in brown and yellow hues, with yellow representing moisture originating from within Colorado. Aquatic sources are depicted in teal and blue, representing contributions from the Atlantic and Pacific Ocean basins, respectively. The bar chart is organized such that contributions from aquatic source regions are all stacked at the bottom, followed by all terrestrial sources on the top for easy differentiation 240 between terrestrial and aquatic contributions. In Figures 3.b and 3.c, the height of the bar charts represents the accumulated monthly volume of evaporation that will fall as precipitation in the Front Range region. Bar height in Figures 3.d and 3.e all add up to 100% to represent the proportion of regional contributions during the specified timeframe. Table 1 contains the explicit values associated with Figures 3.b-e. Table 1 does not provide new information beyond what is shown in Figures 3.b-e, but it does provide the exact values that can be hard to extract from them. It is important to note that we combine contributions 245 from FTR and Colorado in the table. Due to our study region being so small, we defined local moisture sources to include all of Colorado.

At the monthly and annual time scale, total tracked evaporation (a spatial sum across all latitude and longitudes) can be considered approximately equivalent to accumulated precipitation (van der Ent and Tuinenburg, 2017; Gimeno et al., 2021). Moving forward, total annual or monthly tracked evaporation may also be referred to as annual or monthly total precipitation, 250 subject to the limitations of ERA5 as outlined above.

As seen in Figure 3.a, precipitation in May-July of 2023 originated from both terrestrial and aquatic sources located predominantly to the west or southwest of the Front Range. On the individual grid cell level, two prominent clusters of higher water vapor contributions emerge around both Colorado and the Gulf of California. Contributions in Colorado generally decrease as you move further away from the Front Range itself, whereas around the Gulf of California, evaporative 255 contributions sharply decrease following the Mexican coastline. Source regions, although close in proximity, can vary dramatically.



260

**Figure 3: a), b), c), d), e) Spatial and monthly variation in moisture sources of Front Range (FTR) precipitation in May, June, and July of 2023. a) Map of evaporative sources of FTR precipitation accumulating from May through July of 2023. b) Monthly regional contribution to the FTR in volume of water vapor ( $m^3$ ). c) Cumulative regional evaporative contribution across May, June and July of 2023 to FTR precipitation in volume of water vapor ( $m^3$ ). d) Monthly regional evaporative contribution as a percent of total monthly evaporative contribution. e) Cumulative regional contribution as a percent of total monthly evaporative contribution. A map defining each of these regions is provided in the supplementary.**



265 **Table 1: Monthly and cumulative absolute evaporative contribution from May-July of 2023. For readability, values are rounded to the nearest million cubic meter. Each row represents a different region, and columns represents different time periods. Evaporative contribution is described in this table as volumes (m<sup>3</sup>) of water vapor. Evaporative contribution is also referred to as tracked evaporation.**

<i>2023 Absolute Evaporative Contribution by Region:</i>				
<i>Regional Tracked Evaporation (millions of m<sup>3</sup>)</i>				
<b>Region</b>	<b>May 2023</b>	<b>June 2023</b>	<b>July 2023</b>	<b>MJJ Cumulatively</b>
<b>All Colorado</b>	278	439	215	932
<b>Midwestern US</b>	112	68	13	193
<b>Southern US</b>	239	83	32	354
<b>Western US</b>	485	558	311	1,354
<b>Other Land</b>	266	242	178	686
<b>Gulf of Mexico (GoM)</b>	155	12	107	275
<b>Atlantic Ocean</b>	228	97	279	604
<b>Gulf of California (GoC)</b>	83	47	50	180
<b>Pacific Ocean</b>	1,017	968	382	2,367
<b>Other Water</b>	38	25	15	79
<b>All Terrestrial Regions</b>	1,381	1,390	748	3,520
<b>All Aquatic Regions</b>	1,523	1,148	833	3,504
<b>All Regions</b>	2,905	2,538	1,581	7,024

270 **Table 2: Regional evaporative contribution in May-July of 2023 as a percentage of total Front Range moisture. Calculated by taking the region’s absolute evaporative contribution, dividing by the total evaporative contribution from all regions, and multiplying by one hundred. Table 2 is interpreted as the percentage of Front Range rainfall that originated from a given region during that timeframe.**

<i>Relative Evaporative Contribution in 2023:</i>				
<i>Percent of All Region Tracked Evaporation (%)</i>				
<b>Region</b>	<b>May 2023</b>	<b>June 2023</b>	<b>July 2023</b>	<b>MJJ Cumulatively</b>
<b>All Colorado</b>	9.6	17.3	13.6	13.3
<b>Midwestern US</b>	3.9	2.7	0.8	2.7
<b>Southern US</b>	8.2	3.3	2.0	5.0
<b>Western US</b>	16.7	22.0	19.7	19.3
<b>Other Land</b>	9.2	9.5	11.3	9.8
<b>Gulf of Mexico (GoM)</b>	5.3	0.5	6.8	3.9
<b>Atlantic Ocean</b>	7.9	3.8	17.6	8.6
<b>Gulf of California (GoC)</b>	2.9	1.8	3.2	2.6



<b>Pacific Ocean</b>	35.0	38.1	24.1	33.7
<b>Other Water</b>	1.3	1.0	1.0	1.1
<b>All Terrestrial Regions</b>	47.6	54.8	47.3	50.1
<b>All Aquatic Regions</b>	52.5	45.3	52.7	49.9
<b>All Regions</b>	100.1	100.0	100.1	100.0

275 Across the 2023 May-July season, terrestrial and aquatic sources were approximately equal in contribution to Front Range precipitation, with terrestrial sources providing slightly more moisture (Figures 3.c and 3.d and Tables 1 and 2). Regionally, the Pacific Ocean was the most important region, accounting for just over a third of all May-July rainfall. Then, followed by the Western US and Colorado source regions. These three regions alone make up two thirds of Front Range precipitation (Tables 1 and 2). Moisture recycling (moisture from within Colorado) accounted for a non-negligible proportion, making up  
 280 over a tenth of rainfall that season. These contributions from Colorado are greater than the combined evaporative contributions from larger regions such as the Midwestern and Southern US (Table 1). Each month within May-July of 2023 experienced variations in both precipitation totals and moisture sources.

May 2023 is characterized as the wettest month of this May-July (MJJ) season including multiple heavy, convective rainfall events occurring within the month (Figure 3.b and Table 1). More precipitation in this period originated from aquatic surfaces rather than terrestrial, but only minimally (Figure 3.b, Table 1, and Table 2). The Pacific Ocean made up over a third of May  
 285 rainfall, and the Western US followed by Colorado were the next largest contributors. Together these regions accounted for around 60% of total rainfall (Table 2). When compared to June and July of 2023, terrestrial sources to the east (Southwestern and Midwestern US) were more actively contributing moisture during this timeframe.

Notably, June 2023 received the most anomalous amounts of precipitation out of all months that year, despite being the second  
 290 wettest month (Table 1). In June, terrestrial sources were responsible for over half of Front Range precipitation with aquatic sources contributing slightly less than half (Table 2 and Figure 3.d). The Pacific Ocean and Western US remained the most contributing regions, and local moisture sources nearly doubled their evaporative contributions to the Front Range from the previous month (Table 1 and 2). In June, these most dominant moisture sources made up over three quarters of Front Range precipitation (Figure 3.b, Figure 3.d, and Table 2). Compared to May, less moisture originated from eastern aquatic and  
 295 terrestrial source regions, such as the Gulf of Mexico and Southern US (Table 1).

Of this extremely wet three-month period, July 2023 received the least precipitation (Figure 3.b and Table 1). This month, aquatic sources slightly dominate over terrestrial regions with the Front Range receiving greater contributions from aquatic source regions in the East (Figure 3.e and Table 2). Again, the Pacific Ocean and followed by Western US were the greatest contributing regions, but the Atlantic Ocean surpasses evaporative contribution from within Colorado. As seen in Figure 3.b  
 300 and Table 1, water vapor received from the Pacific reduces by half while moisture from the Gulf of Mexico and Atlantic Ocean returns to similar amounts as contributed in May of 2023.



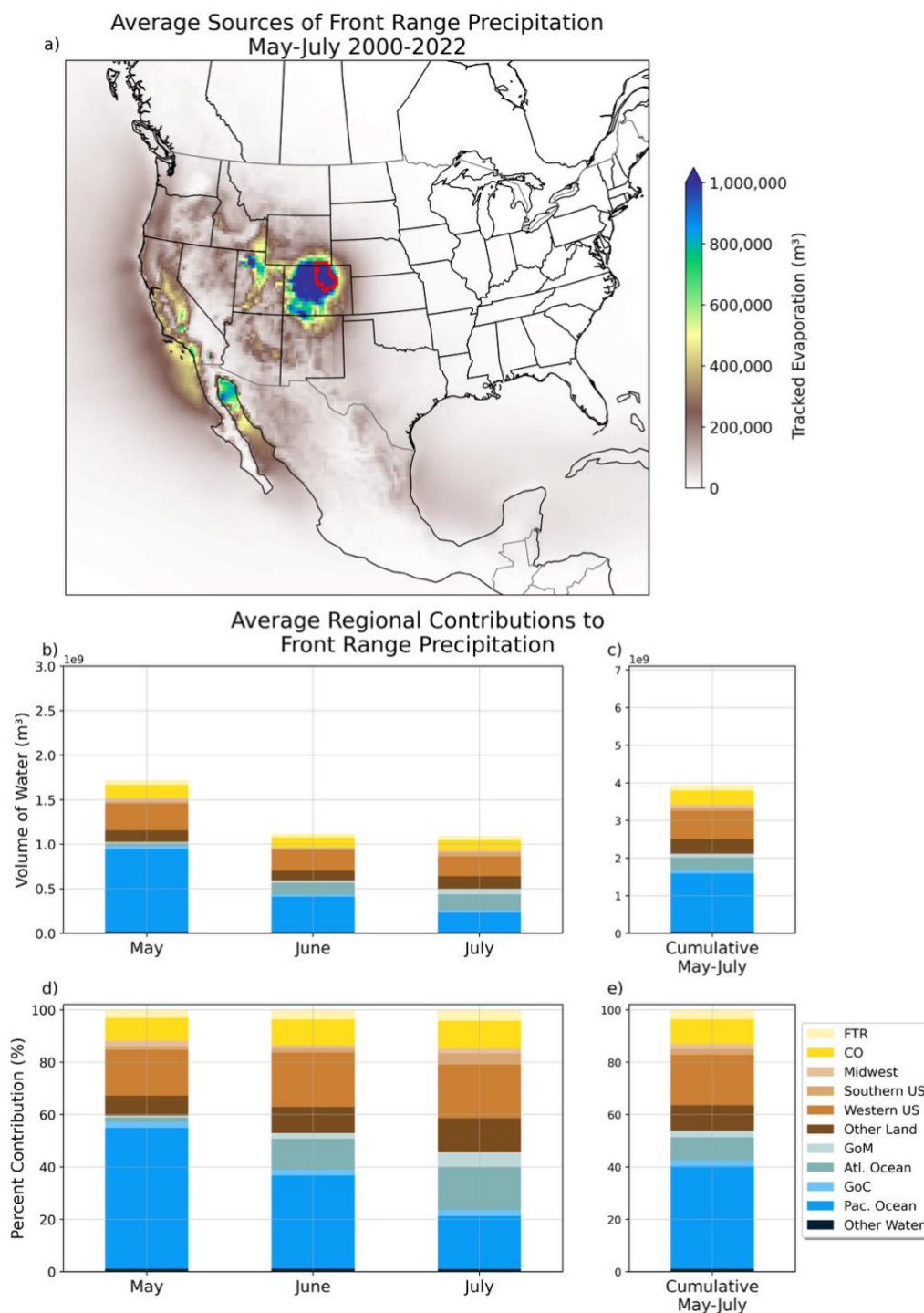
Overall, this section establishes the moisture sources of Colorado's Front Range associated with extreme rainfall during May, June, and July of 2023. Although moisture sources across these three months shifted in terms of direction and water vapor contributed, the Pacific Ocean and Western US consistently dominated Front Range precipitation origins seasonally as well and sub-seasonally.

### 3.2 Comparing 2023 to previous decades

The previous subsection established the moisture sources of extreme rainfall in May, June, and July of 2023 in the Front Range region. This section describes the Front Range's average moisture sources from 2000-2022 (Figure 4.a-e) and compares moisture sources observed in May-July of 2023 to the climatological average. We compare moisture sources in these two different timeframes by examining regional differences in total (absolute) evaporative contribution (Table 3) and relative evaporative contribution (proportional share of total precipitation) (Table 4). Averaging the past twenty-three years of evaporative contributions together highlights consistent moisture sources of Front Range precipitation and provides a baseline to contextualize the moisture sources observed in May-July of 2023 against. It is important to note that when comparing one year against an average, there will be inherent differences, so minor departures from the mean should be taken with caution.

Over the last twenty-three years, rainfall in May-July originated predominantly from aquatic and terrestrial areas directly to the west and southwest of the FTR (Figure 4.a). Specific areas at the grid cell level emerge as consistent and major contributors to Front Range precipitation overall. Figure 4.a demonstrates that areas within Colorado, the Gulf of California, the Pacific Ocean, and Utah are consistent contributors to Front Range precipitation over the past twenty-three years. Comparing Figures 4.a and 3.a, most precipitation in May-July in 2023 originated from these same major source regions, but precipitation overall originated from a broader range of directions.

Considering the surface type (terrestrial or aquatic) of moisture sources, historically, just over half of Front Range precipitation in May-July originates from aquatic moisture sources opposed to terrestrial surfaces (Figure 4.e and Table 4). In May-July of 2023, the proportion of precipitation that originated from terrestrial and were nearly equal. As shown in Table 3, both terrestrial and aquatic sources supplied more amounts of moisture to the Front Range during May-July 2023 than on average (Figure 3.c, Figure 4.c, Table 3). Specifically, terrestrial regions provided nearly twice their average amount, compared with about one and a half times for aquatic regions (Table 3).



330 **Figure 4: (a), (b), (c) Spatial and monthly variation of Front Range (FTR) moisture sources on average from 2000-2022. (a) Map of average tracked evaporation accumulating from May through July. (b) Average monthly regional contributions to the FTR in**



volume of water vapor (m<sup>3</sup>). (c) Average cumulative regional contribution across May, June and July to FTR precipitation in volume of water vapor (m<sup>3</sup>). A map defining each of these regions is provided in the supplementary material.

335 **Table 3: Regional moisture contribution in May-July 2023 relative to average evaporative contribution. Table values are described specifically as the percent of average regional evaporative contribution (tracked evaporation) in May-July of 2023. Calculated by taking the regional absolute evaporative contributions in 2023 (Table 1), dividing them by the average evaporative contribution from 2000-2022, and multiplying by one hundred. In this table, one hundred percent is interpreted as in 2023, regional contribution was exactly average for that month or three-month period.**

<i>2023 Regional Evaporative Contribution Relative to Average: Percent of Average Regional Tracked Evaporation (%)</i>				
<b>Region</b>	May 2023	June 2023	July 2023	MJJ Cumulatively
<b>All Colorado (FTR + CO)</b>	138.1	288.9	133.2	181.1
<b>Midwestern US</b>	299.5	501.7	57.2	263.7
<b>Southern US</b>	991.7	444.8	69.4	401.1
<b>Western US</b>	161.1	241.2	138.7	179.0
<b>Other Land</b>	203.3	216.9	125.6	178.6
<b>Gulf of Mexico (GoM)</b>	1,142.4	50.1	174.0	276.0
<b>Atlantic Ocean</b>	774.6	72.9	155.9	177.2
<b>Gulf of California (GoC)</b>	215.1	188.8	195.0	202.0
<b>Pacific Ocean</b>	109.9	242.6	172.5	153.1
<b>Other Water</b>	209.1	198.2	140.9	188.1
<b>All Terrestrial Regions</b>	198.7	263.7	125.7	193.7
<b>All Aquatic Regions</b>	148.4	193.6	167.2	165.5
<b>All Regions</b>	168.7	226.6	144.6	178.5

340 **Table 4: Relative regional evaporative contribution of each source region on average and in 2023. Values shown in the 2023 columns are from Table 2 and are included for quick reference between average and 2023.**

<i>Relative Evaporative Contribution in 2023 and on Average: Percent of All Region Tracked Evaporation (%)</i>								
<b>Region</b>	<b>May</b>		<b>June</b>		<b>July</b>		<b>MJJ</b>	
	<i>Avg.</i>	<i>2023</i>	<i>Avg.</i>	<i>2023</i>	<i>Avg.</i>	<i>2023</i>	<i>Avg.</i>	<i>2023</i>
<b>All Colorado (FTR + CO)</b>	11.7	9.6	13.6	17.3	14.8	13.6	13.1	13.3
<b>Midwestern US</b>	2.2	3.9	1.2	2.7	2.0	0.8	1.9	2.7
<b>Southern US</b>	1.4	8.2	1.7	3.3	4.2	2.0	2.2	5.0
<b>Western US</b>	17.5	16.7	20.7	22.0	20.5	19.7	19.2	19.3
<b>Other Land</b>	7.6	9.2	10.0	9.5	13.0	11.3	9.8	9.8



<b>Gulf of Mexico (GoM)</b>	0.8	5.3	2.2	0.5	5.6	6.8	2.5	3.9
<b>Atlantic Ocean</b>	1.7	7.9	11.8	3.8	16.4	17.6	8.7	8.6
<b>Gulf of California (GoC)</b>	2.3	2.9	2.2	1.8	2.3	3.2	2.3	2.6
<b>Pacific Ocean</b>	53.8	35.0	35.6	38.1	20.2	24.1	39.3	33.7
<b>Other Water</b>	1.1	1.3	1.1	1.0	1.0	1.0	1.1	1.1
<b>All Terrestrial Regions</b>	40.4	47.6	47.1	54.8	54.4	47.3	46.2	50.1
<b>All Aquatic Regions</b>	59.6	52.5	53.0	45.3	45.6	52.7	53.8	49.9
<b>All Regions</b>	100.0	100.0	100.0	100.0	100.0	100.0	100.0	100.0

When considering the geographical regions responsible for average Front Range precipitation, the Pacific Ocean region contributed the greatest amount of water vapor, followed by the Western US and Colorado regions. Together they account for just under three quarters of average precipitation. In comparison, dominant moisture source regions during the May-July 2023 season were the exact same (Figure 3.c and Table 4). Interestingly, as seen in Figure 5, less dominant source regions, such as Southern US, Midwestern US, and Gulf of Mexico, contributed up to four times that amount of water vapor they typically do and accounted for a greater proportion of MJJ rainfall than the last 23 years.

May-July of 2023 Percent of Average Contribution to Front Range Precipitation

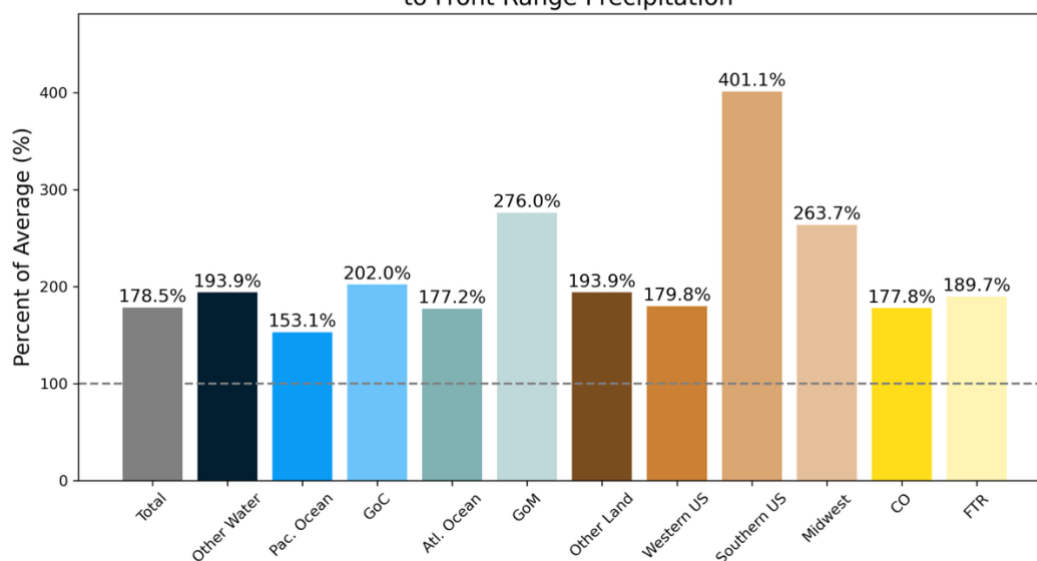


Figure 5: Regional percent of average contribution in May-July of 2023. Grey dashed line is plotted at 100% of average differentiating between regions that contributed more than average (> 100%) and regions that contributed less than average (< 100%) to precipitation in the May-July of 2023 season. Each color represents a different source region.



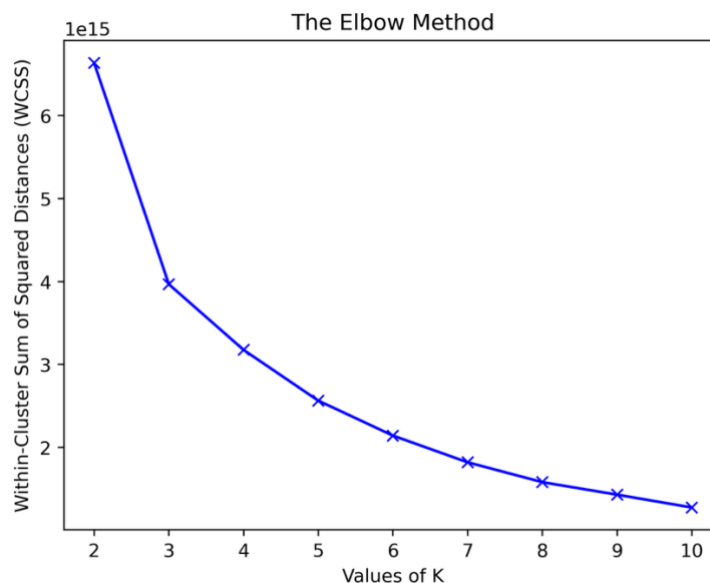
355 To briefly summarize this section, precipitation in May-July of 2023 originated from a broader range of regions when compared to the past twenty-three years on average. The Front Range received more total moisture from all source regions, with the Pacific Ocean, Western US, and Colorado responsible for most of the anomalous precipitation during this extremely wet season. Contributions from eastern regions such as the Southern US, Midwestern US, and Gulf of Mexico delivered up to four times the amount of water they usually do but were not responsible for most of the anomalous precipitation.

### 3.3 Clustering of Interannual Evaporation Patterns

To further contextualize the moisture sources in 2023 with individual years, we applied a k-means clustering analysis to May-July tracked evaporation anomalies from 2000-2023. By doing so, we hope to identify whether source regions during the 2023  
360 May-July season align with other anomalously wet May-July seasons rather than comparison to the average.

As stated in the methods section, we use the elbow method to partially determine the number of clusters to use for this analysis. The elbow method is one of the most popular methods used to determine optimal k values. This method is often criticized for its subjectivity when the ‘crook’ of the elbow is not well defined. However, as seen in Fig. 6, we believe the crook of the elbow is clear and well defined. This method identifies the optimal number of clusters by calculating the within-cluster sum of the  
365 squared errors (WCSS) between all samples and their identified centroid. The optimal cluster number is apparent when adding more clusters does not significantly reduce the WCSS significantly (Syakur et al., 2018). As shown in Figure 6, after k values of three or four, WCSS decreases minimally. As such, we decided to use three clusters in efforts to strike a balance between model simplicity and capturing meaningful structure in the data.

This analysis was also conducted for k values of 4 and 2 to ensure that the main characteristics of clusters did not change  
370 dramatically when choosing a different k value. We found very similar clusters when using a k value of 4, with nearly identical clusters to those found here with an added cluster of one MJJ season, May-July of 2015. When using a k value of 2, the MJJ season were sorted into clusters that resembled the wet and dry clusters shown in Figure 7 with May-July of 2023 being sorted into the cluster with a composite of positive tracked evaporation anomalies around Colorado. The characteristics between clusters found in this section did not change dramatically when altering the number of k values.



375

**Figure 6: The elbow method with within-cluster sum of the squared error on the y axis and k, the number of specified clusters, plotted on the x axis. Before WCSS was calculated, the centroid clusters were calculated iteratively 100 times.**

K-means clustering was used to group the twenty-four MJJ seasons from 2000 to 2023 into three distinct categories with similar spatial patterns. Figure 7.a-c describes the average MJJ tracked-evaporation anomaly pattern for each cluster. Figure 380 7.d is a time series of the spatially summed tracked evaporation for a given MJJ. At the 3-month timeframe, total tracked evaporation is also equivalent to total precipitation (van der Ent and Tuinenburg, 2017; Gimeno et al., 2021). Each MJJ is then colored by what cluster they were assigned to.

Clusters one and two represent years with generally increased or decreased moisture contributions from Colorado, along with modest shifts in contributions from the Pacific Ocean, Gulf of California, and Western US (Figures 7.a and 7.b). From analysis 385 in Sect. 3.2, these regions closely coincide with major moisture sources of Front Range precipitation. Figure 7.d describes the years assigned to each cluster as well as the total Front Range precipitation associated with that given season.

MJJ of 2023 was the only year assigned to cluster three (Figure 7.d), making it an outlier in this 24-year record. As a result, the centroid in Figure 7.c reflects only 2023's tracked evaporation anomalies and is not a composite of multiple years. Although 2023 shared the same dominant moisture sources (e.g. Colorado and the Pacific Ocean), the magnitude of contributions from 390 those regions was dramatically higher than in any previous year (figure 7.d).

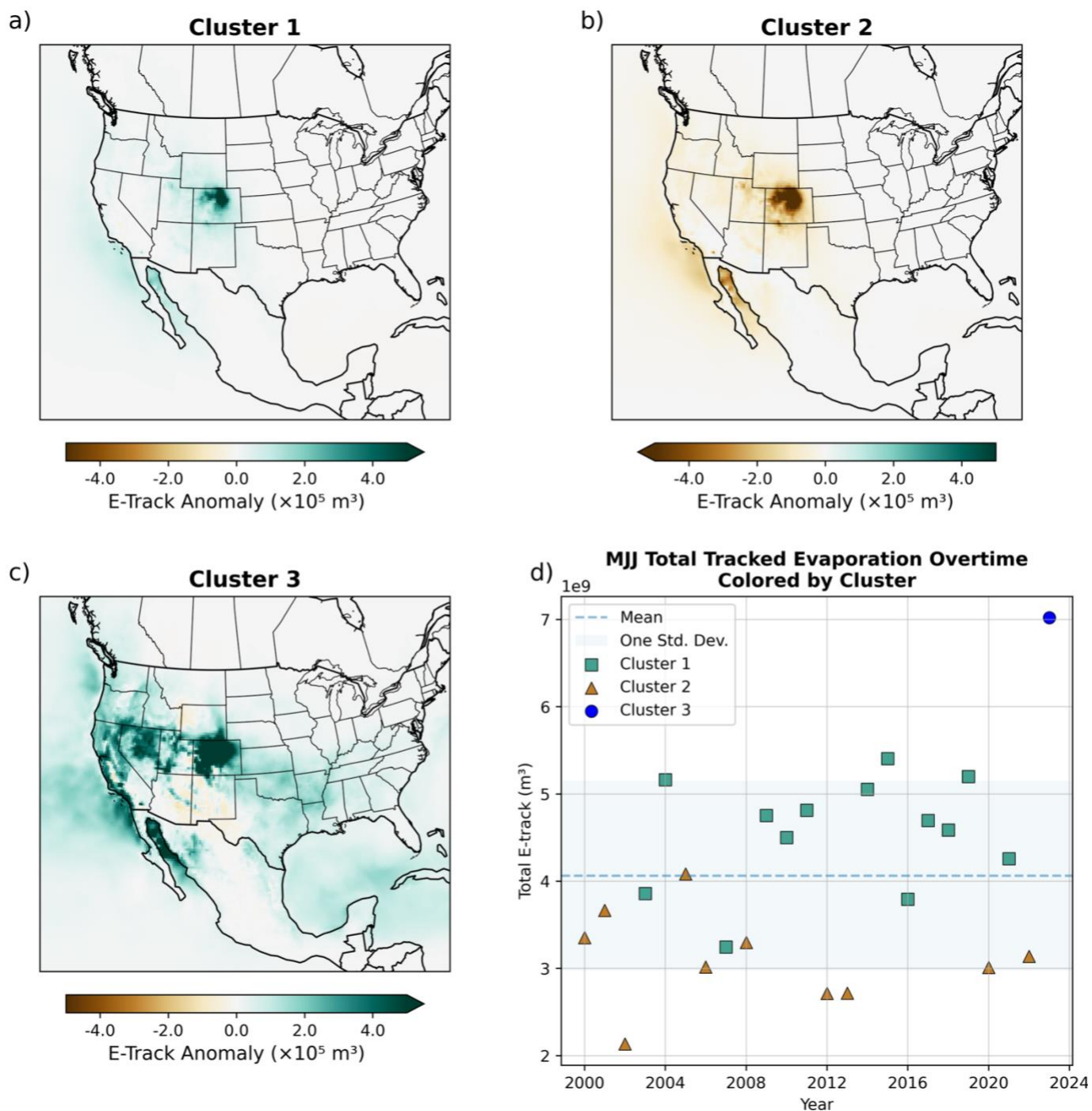
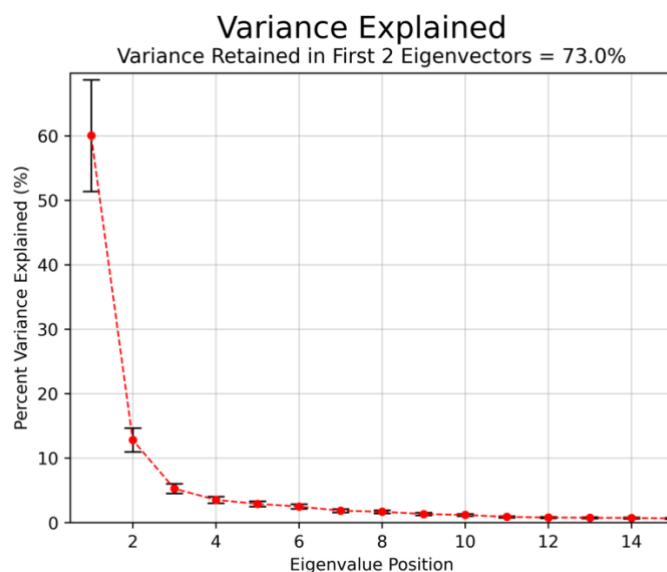


Figure 7: Spatiotemporal patterns of MJJ evaporation anomalies from k-means Clustering. (a), (b), (c) Cluster average MJJ moisture contribution. (d) MJJ total precipitation (spatially summed e-track) plotted overtime. Color and shape assigned by cluster number.



### 3.4 Dominant Variability Patterns

In this last section of analysis, we identify the dominant variability patterns of MJJ season moisture sources using an empirical orthogonal function (EOF) analysis. Figure 8 illustrates the percent of variance explained (PVE) by a given eigenvector sorted from most to least variance explained. This value is determined by dividing the eigenvalue of a given eigenvector by the sum of all eigenvalues and multiplying by one hundred.



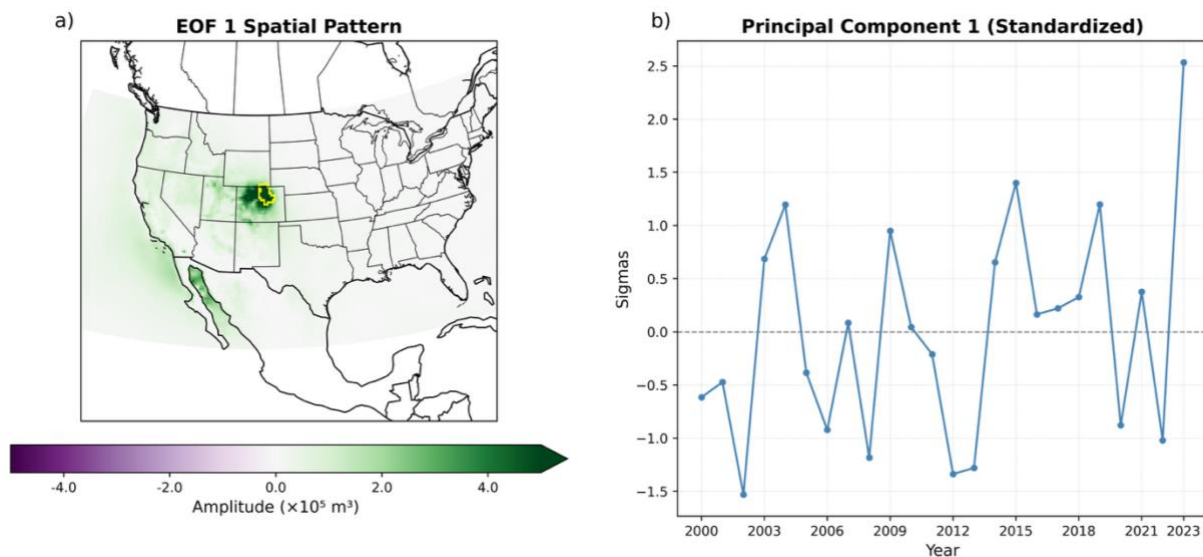
**Figure 8: Percent variance explained (PVE) by eigenvectors ranked from least to greatest eigenvalue. Error bars represent 95% confidence bounds as calculated in North et al. (1982) assuming that each MJJ season is independent of one another.**

In this analysis, we only discuss the first two eigenvectors which together account for 72.0% of the variance in MJJ season tracked evaporation from 2000 to 2023. Separately, eigenvector one accounts for 60.0% of variance and with 95% confidence, it could range from 68.7% to 51.4% of variance in our data. Eigenvector two accounts for 12.8% of variance and its confidence bounds range from 14.7% to 11.0%. By convention, eigenvector one represents the most variance in the system, but it accounts for much more variance than all the other eigenvectors (i.e. vectors 2-28,245) combined. As seen in Figure 8, after eigenvector two, percent variance explained decreases very little with increases in each subsequent eigenvector. As such, this analysis only focuses on the first two eigenvectors and their associated principal components.

As seen in Figure 9.a, the first eigenvector (EOF1) describes a pulsing of positive and negative tracked evaporation anomalies from within Colorado, the Pacific Ocean, and Gulf of California. The highest evaporation contribution anomalies occur within the sink region itself, extending beyond the colorbar range plotted. This eigenvector accounts for the largest portion of variance in the data, representing the dominant mode of variability among MJJ seasons from 2000 to 2023. Figure 9.b shows the normalized principal component (PC1) associated with eigenvector one. Essentially, the values in PC1 represent how much of



the spatial pattern shown in EOF1 is in a given year. The MJJ season of 2023 has the strongest expression of EOF1 with over 2.5 standard deviations above the average.



420 **Figure 9: (a) Spatial pattern of the first empirical orthogonal function (EOF1) of MJJ tracked evaporation anomalies for the Front Range region (FTR) from 2000–2023. (b) Standardized principal component time series (PC1) corresponding to EOF1.**

While EOF1 mainly represents the pulsing behaviour of Colorado moisture contribution, EOF2 describes a north-south dipole pattern in anomalous tracked evaporation as seen in Figure 10.a. This spatial pattern implies that years with large positive values in PC2 (Figure 10.b) received anomalously high amounts of moisture from Western US and anomalously low amounts of moisture from the Pacific Ocean and the Southwestern US. The most intense tracked evaporation anomalies still reside within Colorado but also expanded to northern Utah and the Pacific Ocean. EOF2 represents 12.8% of the variance in evaporative contribution in MJJ, considerably less than EOF1, but nonetheless represents the secondary mode of variability in our data. In 2023, PC2 value is only 0.2 standard deviations away from the average. Since the PC2 value in 2023 is near zero, this secondary mode of variability had little role in the 2023 MJJ season precipitation.

430 This EOF analysis reveals the two dominant modes of moisture source variability among the past twenty-four MJJ seasons and which modes were more important in precipitation observed in May-July 2023. The dominant mode of variability in our dataset, EOF1, was a pulsing behaviour depicting whether a given year had anomalously high or low contributions from Colorado, the Gulf of California, and the Pacific Ocean. The positive phase of EOF1 indicating increased evaporative contributions from these regions played a significant role in 2023 compared to other years. In contrast, the secondary mode of variability, EOF2, describes a dipole between northern and southern moisture sources and had much less of a role in 2023.

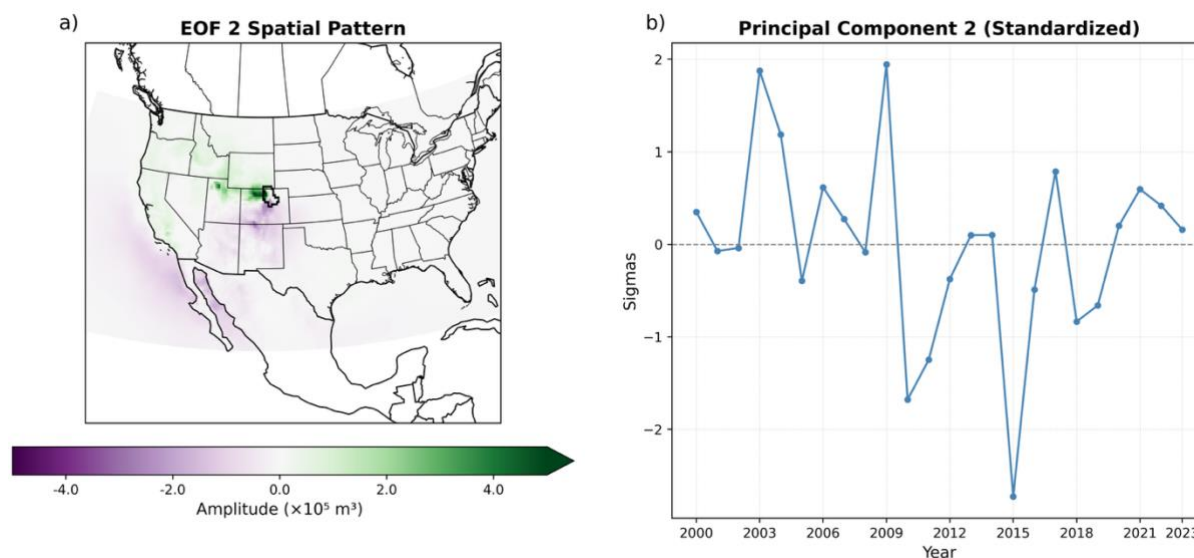


**Figure 10: (a) Spatial pattern of the second empirical orthogonal function (EOF2) of MJJ tracked evaporation anomalies from 2000–2023. (b) Standardized principal component time series (PC2) corresponding to EOF2.**

#### 440 4. Discussion

In summary, this study provides new insights into the moisture sources of Colorado’s Front Range precipitation during May–July, and more specifically for the 2023 season. Section 3.1 identified the Pacific Ocean, Western US, and Colorado as the primary origins of two thirds of the extreme precipitation in May–July of 2023. Since the Front Range sits in a location influenced predominantly by upper-level westerly winds, it is somewhat expected that major moisture sources were located to the west of our sink region (Doesken et al., 2003). Section 3.2 found that the origins of 2023’s extreme precipitation were dominated by typical source regions. The implications of these findings suggest that the extremely wet conditions in May–July of 2023 likely occurred due to abnormally large amounts of water vapor from the Pacific Ocean, Western US, and Colorado reaching and converging upon the Front Range region rather than being driven by an anomalous influx of moisture from an atypical location. In this case, anomalous contributions from the Southern US, Gulf of Mexico, and the Midwest may have only acted to enhance the already anomalous evaporative fluxes reaching the Front Range from major source regions. Thus, we could not identify potential source regions that could be responsible for extreme precipitation in the Front Range. Furthermore, although moisture contributions from local, terrestrial sources increased in May–July of 2023, their proportion to overall rainfall was roughly the same as aquatic counterparts. Thus, we cannot conclude that local, terrestrial sources were substantially important to the wet May–July conditions observed in 2023.

450 To thoroughly evaluate the uniqueness of May–July 2023, it was also important to evaluate the moisture sources of prior, individual seasons. This allowed for comparison beyond a long-term average and highlights whether 2023 reflects typical variability or a distinct departure from prior moisture sources. Section 3.3 identified moisture sources in the 2023 season as an



analytical outlier among the past twenty-three years by sorting it into a cluster of its own. While the spatial pattern of source region remains consistent with climatological norms found in previous sections, the volume of these contributions likely varied enough to distinguish 2023 entirely. Even when compared to individual years, May-July of 2023 was truly unique and unable to be contextualized with other wet seasons in the previous twenty-three years (2000-2022). Further inhibiting our ability to identify source regions that could potentially enhance our early warning capacity for events like observed in May-July of 2023. Finally, section 3.4 identified two dominant patterns of variability associated with May-July moisture sources. The 2023 season can be understood as an extreme expression of the dominant mode of variability throughout 2000-2024. This dominant mode of variability highlights tracked evaporation anomalies originating from Colorado, the Pacific Ocean, and the Gulf of California, this could suggest that anomalous moisture contributions to the Front Range typically arise from large-scale increases across these regions rather than from localized shifts in individual sources. Although the second EOF could potentially provide predictive insight during wetter or drier seasons, it is considered relatively less important to the moisture sources in the 2023 season and lies outside the scope of this project. To understand the physical basis of EOF2, more research would need to be conducted looking at the prominent synoptic environment within years with strong positive or negative PC2 values. To speculate, EOF2 could represent the movement of the subtropical jet stream altering north-south moisture sources from latitudinal movement, or the variability in the North American Monsoon circulation which could lead to increased/decreased contributions from the American Southwest and Pacific Ocean.

Due to the recency of the 2023 events, our conclusions were somewhat more difficult to corroborate since no peer-reviewed studies had been published on these same events at the time of this writing. There is, however, literature examining moisture sources during historically wet seasons for the entire Southwestern United States (including Colorado). Based on this, we can qualitatively review how 2023 moisture sources compare broadly to sources during other wet years. Skinner et al. (2023) found that during the wettest summers (June, July, August) in the Southwestern United States, the percent change in moisture from areas inside the region compared to normal increased by 42% and from areas outside of the Southwest, increased by 48% (Skinner et al., 2023). This could suggest that during wet years in the Southwest, there is a widespread increase in moisture content from nearly all source regions, rather than a singular anomalous import from a specific source region. Our findings indicate a similar pattern. We found that Colorado's northern Front Range received anomalously high precipitation contributions from all dominant moisture source regions. To truly understand the potential mechanism of enhanced wet season precipitation, additional modelling and analysis beyond the scope of this work would be required.

Our understanding of the northern Front Range's typical moisture sources aligns with and contrasts various findings in existing research. McKee et al. (2000) states that the statewide primary sources of summertime precipitation in Colorado strictly come from aquatic sources such as the Pacific Ocean, the Gulf of Mexico and the Gulf of California. Our results concur that the Pacific Ocean is the greatest moisture source by volume for the Front Range in May, June, and July, but we also find that the western US and Colorado itself are some of the major sources of moisture. We also affirm that aquatic sources all together make up over 50% precipitation on average and consider aquatic source regions to be more dominant source of moisture to Front Range precipitation than terrestrial sources on average (Figure 4.e).



495 However, our study indicates that the Gulf of California and the Gulf of Mexico are considered minor moisture sources in terms of volume, only making up 2.3% and 2.5% of MJJ precipitation on average. It is important to note that compared to the entire Pacific Ocean, the Gulf of California and the Gulf of Mexico are much smaller in area. Although they do not make up a major source of precipitation by volume, they can contribute a lot of water vapor per unit area. McKee et al. (2000) did not provide quantitative estimates of moisture sources for Colorado nor the Front Range specifically, so we are unable to directly compare results. Nonetheless, we do find general agreement in the prominence of large-scale aquatic sources, particularly the Pacific Ocean, as major contributors to MJJ precipitation in Colorado. Another likely source of discrepancy could be how we define evaporative contributions from sources. Since we define moisture sources by where precipitation last evaporated from, these regional contributions do not include moisture that initially evaporated from the Gulf of Mexico or Gulf of California but later precipitated and reevaporated again before reaching the Front Range.

500 Jana et al. (2018) used the Lagrangian particle tracking model, HYSPLIT, to trace the moisture trajectories of precipitation falling at a point location in Eastonville, Colorado (south of the Front Range region) from 1979–2013. This study found evidence that the dominant source of moisture in eastern Colorado is almost exclusively land evaporation followed by modest amounts from the Gulf of California (Jana et al., 2018). In contrast, our study found that on average, terrestrial sources make up 46.2% in the Front Range which sits just north of Eastonville. Since these regions do not overlap, we expect some discrepancies in moisture sources, but due to the proximity of these areas, it is interesting that Eastonville appears to receive a much larger proportion of its rainfall from terrestrial sources.

510 One likely reason for this is that the Jana et al. (2018) study traced moisture backwards only for 3 days before the precipitation event. It is possible that the moisture from other sources identified in our study, such the Pacific Ocean or Atlantic Ocean, surpasses the three-day tracking limit for the HYSPLIT simulations, and so was excluded from consideration of this study. As mentioned before, water vapor has an average residence time of under nine days (van der Ent et al., 2014), so considering the Front Range's distance from oceanic bodies of water, it is reasonable to expect water from aquatic sources to take longer than 3 days to travel to Colorado.

515 Our finding that terrestrial regions contributed a greater proportion of total precipitation during this specific wet year in Colorado's Front Range, is consistent with observations from other studies of wet years in the Southwest. The Skinner et al. (2023) study discussed earlier in this section found that during the wettest Springs (March, April, May), 14–18% of springtime precipitation in the Southwestern United States originated from inside the region itself (Skinner et al., 2023). Whereas during the wettest summers, recycled moisture made up 30% of Southwestern precipitation. These estimates are higher than the proportion FTR contributes to its own precipitation in May, June, and July of 2023 as shown in Figure 3.c. Given that moisture recycling is very dependent on the selected study region (van der Ent et al., 2010), it is understandable that the paper by Skinner et al. (2023) has a different proportion of moisture recycling due their study region covering a much broader area, spanning multiple states.

525 In terms of the possible importance of land evaporation during wet years, Erlingis et al. (2019b) suggests that in Colorado and New Mexico, summer precipitation in wetter years is prominently influenced by land surface evaporation (Erlingis et al.,



2019b). Yet, more research is needed to truly understand the relationship between terrestrial sources of moisture and extreme precipitation.

Finally, we consider the results of our EOF analysis to assess dominant patterns of moisture source variability in Front Range precipitation from 2000 to 2023. As mentioned above, the lack of studies directly analysing this event or region limits direct  
530 corroboration, so we interpret our results in the broader context of related work on large-scale moisture source variability. In Keys et al. (2014), they find that for three distinct sink regions in China, Africa, and South America, the greatest year-to-year variability in core moisture sources is characterized by a pulsing pattern of increased or decreased evaporative contributions. This finding remains true even when using a different reanalysis dataset, MERRA (Keys et al., 2014). For the Front Range, we reach the same conclusion that interannual variability in Front Range moisture sources can best be described by pulsing of  
535 anomalous contributions from high-contributing source areas, as illustrated by EOF1 in Figure 9.a.

#### 4.1 Future Work

As mentioned previously, moisture sources are unique and depend on the selected study region and period. Thus, the results discussed above would be difficult to apply to other regions outside of eastern Colorado that differ in size and location compared to the Front Range. However, the methodology and approach used in this study are versatile and can be applied  
540 anywhere hydroclimatic extremes occur. This approach systematically relates a given extreme season against its recent historical moisture sources to better understand moisture transport and potentially identify source regions associated with hydroclimatic extremes. We would encourage other researchers to apply our approach to a given region and period of interest to ultimately better contextualize and potentially predict extreme precipitation around the world.

Future research could also benefit from a more detailed examination of the specific atmospheric pathways that moisture takes  
545 to the Front Range and the specific synoptic drivers associated with transporting water vapor. Since the origin of precipitation in the Front Range primarily remained the same in 2023 compared to average, increased predictability of this event cannot come from moisture source identification and comparison to average conditions alone. Further investigation of anomalous evaporation and circulation anomalies is needed to discern whether these source regions simply evaporated more moisture into the atmosphere overall or whether increased atmospheric pathways from these regions to the Front Range was more responsible  
550 for the excess in water vapor arriving in our study region. Understanding the precise transport mechanisms such as low-level jets, the North American Monsoon, and upslope flows could provide key insights into the drivers of extreme precipitation in Colorado and increase forecast ability of extreme precipitation events in Colorado. Additionally, investigating the links between large-scale teleconnections and moisture source variability would also improve our understanding of how climate modes (e.g. ENSO) regulate moisture transport to the Front Range.

Furthermore, the distinctiveness of 2023 emerging as a cluster of its own highlights how abnormally intense the moisture  
555 inflow was, despite the familiar major source regions. This raises compelling questions about the cause of such intense moisture transport. Future research could examine the dynamical drivers behind moisture transport in the early summer of 2023.

Although such interpretation is beyond the scope of this project, the isolation of 2023 underscores the value of moisture source tracking in identifying and contextualizing the nature of extreme hydroclimatic events.

560 Additionally, this study's results are limited to the reliability of our input data, the ERA5 Reanalysis datasets. Thus, contextualizing these results with observational datasets such as stable water isotope analysis or satellite-based water vapor observations can corroborate the moisture sources found in this study.

Due to project time-constraints, our moisture source analysis was limited to tracked evaporation data from 2000 to 2023. Continuing the analysis period beyond the twenty-four years used in this study could reveal whether moisture source patterns  
565 in May-July of 2023 represent an increasingly relevant trend or simply an anomalous outlier for the Front Range. A longer-term dataset would also strengthen the robustness of the results presented here.

Although our analysis focuses on moisture sources of seasonal and monthly precipitation, the WAM2layers model does provide moisture source data at smaller timescales. Finer time resolution analyses sit outside the scope of this work but understanding the moisture sources of individual events or at the sub monthly time frame can provide important insights into  
570 how moisture can be transported to and from the Front Range for individual high impact events.

## 5. Conclusions

Focusing on Colorado's most populous regions, this research provides a comprehensive analysis on the moisture sources associated with the extremely wet May-July season of 2023. Utilizing ERA5 reanalysis data and the WAM2layers model, we provide insight into the recent evaporative origins of warm-season precipitation in Colorado's Front Range. This  
575 extraordinarily wet May-July appears to result from an anomalous increase in water vapor contributions from typical dominant source regions, with terrestrial sources and regions within Colorado playing an unexpectedly larger role than usual in the 2023 season. With these typical source regions likely driving much of the inter-annual variability in moisture sources, these findings highlight the Front Range's possible sensitivity to land-atmosphere feedback processes or changes in the evaporative fluxes of local land surface. Specifically, this work demonstrated the following key findings for the evaporative origins of the 2023  
580 May-July season:

1. The three primary moisture sources were the Pacific Ocean, Western US, and Colorado, accounting for just over 66.2% of total precipitation.
2. Historically, those same source regions dominate evaporative contributions in May-July, but terrestrial contributions and local moisture recycling (i.e., precipitation that recently evaporated from within the Front Range) in May-July of  
585 2023 accounted for a slightly greater proportion of precipitation than on average.
3. Moisture sources in May-July 2023 were a statistical outlier in terms of the magnitude of moisture contributed to the Front Range, forming a cluster of its own relative to the past 24 years.
4. Between the two most dominant modes of variability, May-July of 2023 aligns more with a basin-wide pulsing pattern rather than a north-south dipole pattern of moisture sources.



590 Ultimately, this work lays the foundation to better understand May-July precipitation in eastern Colorado and provides novel insights into the evaporative sources during the extremely wet May-July 2023 season. Addressing the evaporative origins of extreme precipitation is one of the first steps in better predicting precipitation extremes in this region, and eventually better preparing communities in the Front Range against damages associated with hydroclimatic extremes.

## Appendix A

### 595 A.1 Comparison between ERA5 and PRISM Monthly Precipitation Totals

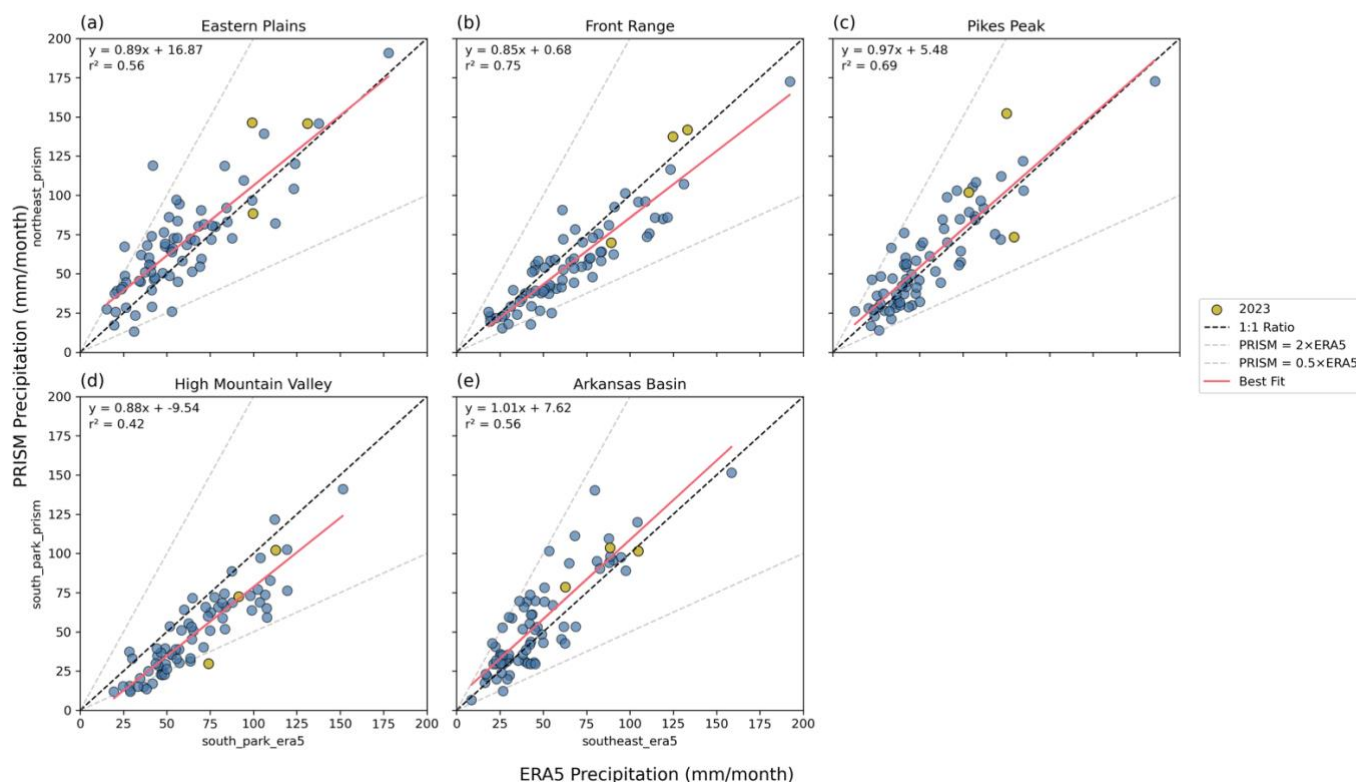
In this study, we rely on the use and accuracy of hourly ERA5 variables such as precipitation, evaporation, u and v wind components, etc. to evaluate the moisture sources of precipitation across eastern Colorado. Since ERA5 precipitation data does not directly assimilate in-situ precipitation observations into its precipitation product and is known to have trouble representing convective precipitation (Hersbach et al., 2020), it is important to ensure that the precipitation product used in this study can capture the anomalously wet conditions observed in May-July of 2023.

600 In this section we compare ERA5 monthly precipitation to the Parameter-elevation Regressions on Independent Slopes Model (PRISM) monthly precipitation originally developed and maintained by researchers within the PRISM Group at Oregon State University. This comparison uses the stable monthly total precipitation estimates from May 2000 to July 2023 and can be downloaded from their website at <https://prism.oregonstate.edu>. The PRISM monthly precipitation dataset is a reasonable choice for comparison due to its gridded nature, incorporation of in-situ precipitation observations, and ability to resolve complex terrains (Daly et al., 2021). The goal of this comparison is to evaluate whether ERA5 captures the anomalously wet conditions observed in May-July of 2023. Since PRISM monthly precipitation has a much finer resolution than ERA5, PRISM monthly precipitation was regridded to ERA5's coarser quarter degree latitude-longitude resolution using xESMF's conservative regridding algorithm (Zhuang et al., 2025).

610 Figure A1 describes the difference in the sink region monthly precipitation accumulation in May, June, or July between ERA5 (x-axis) and PRISM (y-axis) precipitation datasets. Figure A2 and A3 highlight the spatial differences between ERA5 and PRISM precipitation datasets across May, June, and July (MJJ).



ERA5 and PRISM Regional Monthly Precipitation Totals  
May, June, and July 2000-2023



615 **Figure A1 Comparison of ERA5 and PRISM monthly precipitation totals summed across source regions (ex. Northeast). Only plotting precipitation totals in the months of May, June, or July. May-July of 2023 is plotted as yellow markers. Best fit line plotted in red and slope, y-intercept, and  $r^2$  value annotated in the top left corner. Dashed lines from left to right represent 2:1, 1:1, and 1:2 PRISM to ERA5 precipitation ratios.**

Our analysis presents the moisture sources of precipitation falling anywhere within these sink regions, so comparing precipitation totals at the regional scale is a natural choice. As seen in fig. A1, precipitation totals across every sink region have a positive and mostly linear relationship between PRISM and ERA5 precipitation estimates. Generally, increasingly wet months in PRISM coincide with wetter months in ERA5, suggesting that ERA5 can represent changes in regional precipitation accumulation, despite coarser resolution and exclusion of in-situ precipitation observations.

620 As shown in Figure A2 there are substantial differences in precipitation accumulation throughout eastern Colorado between the two datasets. However, when we standardize precipitation amounts relative to each dataset's long-term average and variability, ERA5 identifies May-July of 2023 as anomalously wet compared to average precipitation patterns. This indicates that although biases exist in ERA5 precipitation estimates, May-July of 2023 is relatively very wet among the past twenty-three years. Since this study focuses on putting the evaporative origins of precipitation in May-July of 2023 into perspective of the past twenty-three years, we believe that ERA5 is well suited for this purpose and the research presented.



630

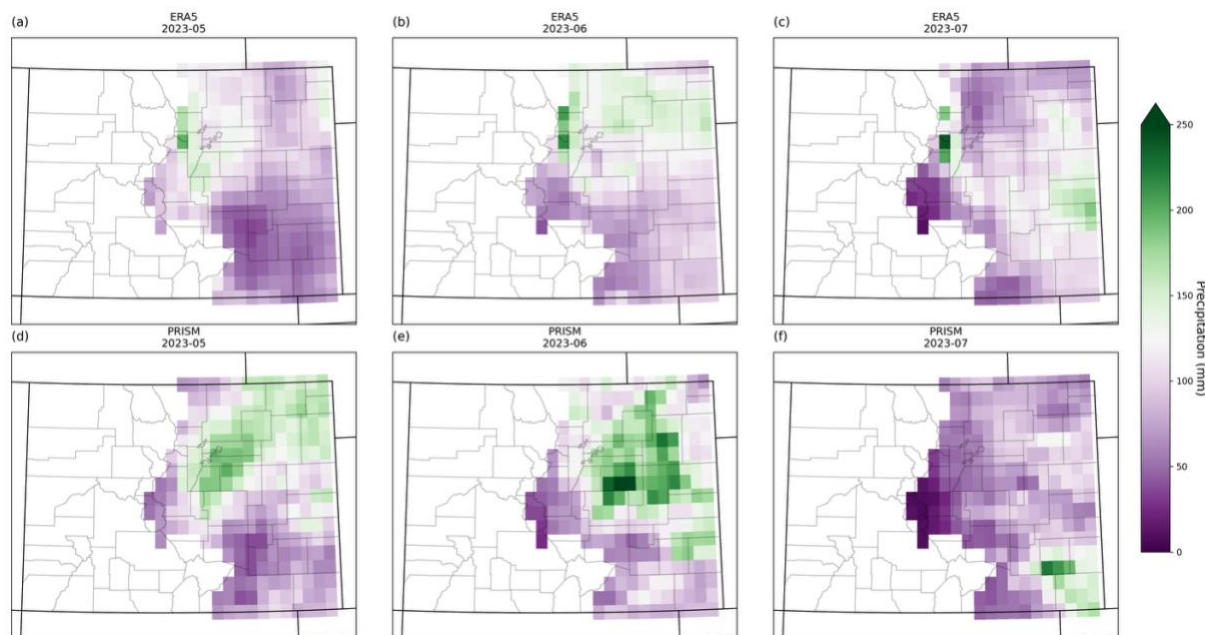


Figure A2 Total monthly precipitation (mm) in eastern Colorado during May-July of 2023. Maps across the first (a-c) row reflect precipitation data from the 0.25-degree latitude-longitude ERA5 Reanalysis dataset. Maps across the second (d-f) row reflect precipitation data from PRISM's Monthly Time Series dataset regridded to a 0.25-degree resolution. Precipitation data is masked to only show precipitation totals over the five sink regions used in this full study.

635

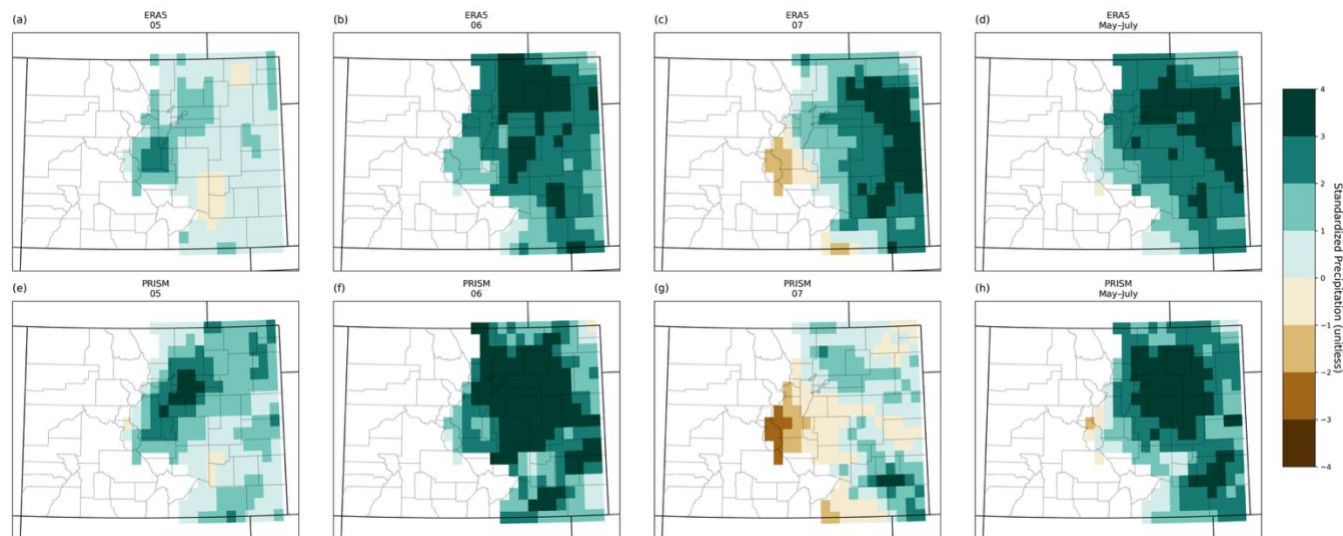


Figure A3 Standardized anomalous monthly precipitation in eastern Colorado during May-July of 2023. These maps indicate how many standard deviations 2023 was from the 2000-2022 average relative their respective datasets. Maps across the top row (a-d) reflect standardized anomalous precipitation from ERA5 whereas the bottom row (e-h) show estimates from the regridded PRISM data. Precipitation data is masked to only show precipitation totals over the five sink regions used in this full study.

640



## A.2 Source and Sink Region Maps

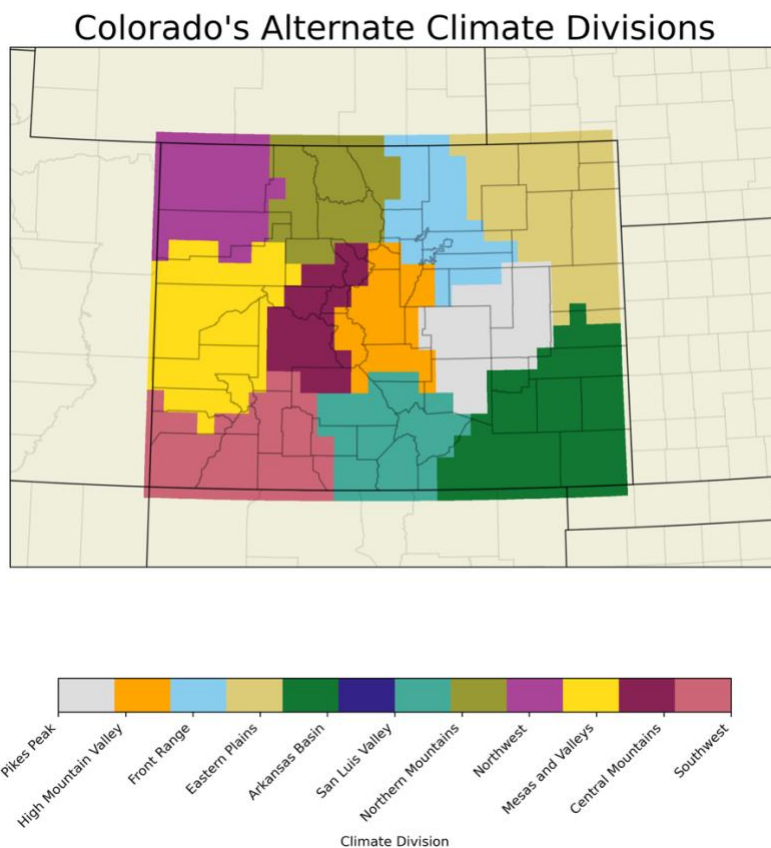


Figure A4: Colorado's alternate climate divisions described in Schumacher et al. (2024) adapted to a 0.25°x0.25° latitude longitude grid. State and county boundaries are marked in black and grey.

## Moisture Source Regions

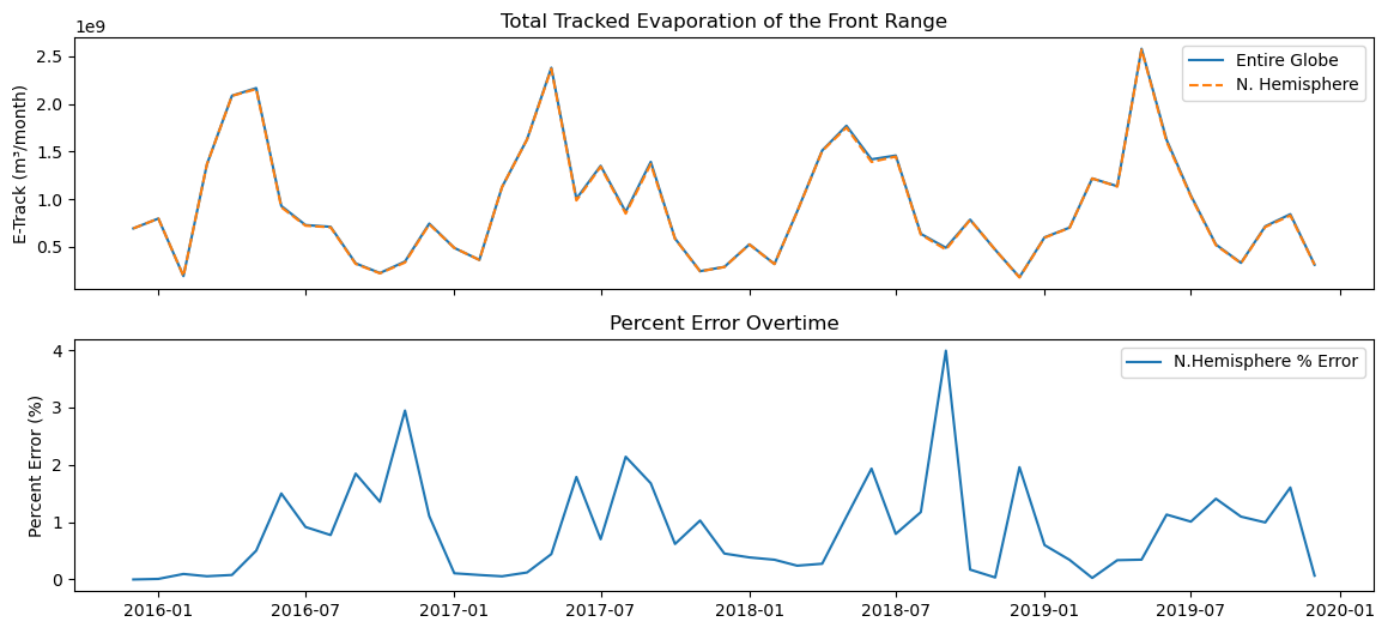


Figure A5: Classification of moisture source regions. Broader ocean areas follow the Global Oceans and Seas dataset (Flanders Marine Institute, 2021), and suboceanic regions, including the Gulf of Mexico and Gulf of California, are defined using International Hydrographic Organization boundaries (Flanders Marine Institute, 2018). Land-based regions are based on the U.S. Census Bureau regional divisions. The sink region shown here is the Front Range, but changes depending on the sink region for each analysis.

645



### 650 A.3 Domain Sensitivity Analysis



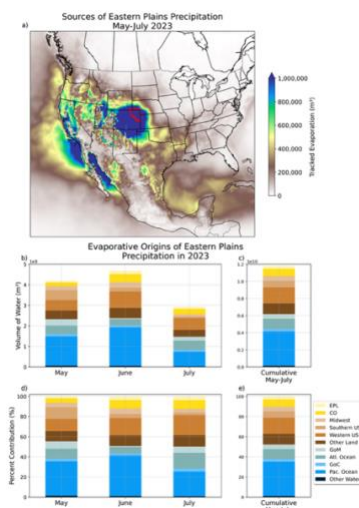
**Figure A6:** Sensitivity analysis comparing the monthly spatially summed tracked evaporation ( $m^3$ ) between WAM2layer runs with different latitude-longitude constraints. The global run tracks evaporation from regions within  $80^{\circ}S$  to  $80^{\circ}N$  latitude whereas the northern hemisphere runs from  $0^{\circ}$  to  $80^{\circ}N$  latitude.

655



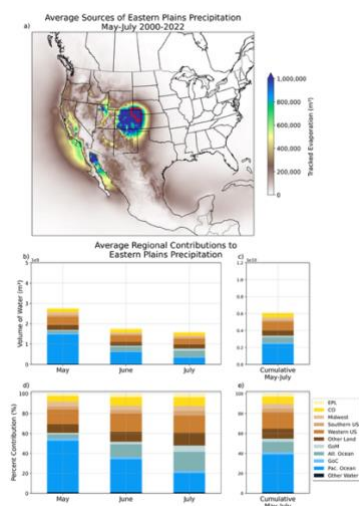
## Appendix B: Other Sink Region Analyses

### B.1 Eastern Plains Region Analysis



660 Figure B1: a), b), c), d), e) Spatial and monthly variation in moisture sources of eastern Plains (EPL) precipitation in May, June, and July of 2023. a) Map of evaporative sources of EPL precipitation accumulating from May through July of 2023. b) Monthly regional contribution to the EPL in volume of water vapor ( $m^3$ ). c) Cumulative regional evaporative contribution across May, June and July of 2023 to EPL precipitation in volume of water vapor ( $m^3$ ). d) Monthly regional evaporative contribution as a percent of total monthly evaporative contribution. e) Cumulative regional contribution as a percent of total monthly evaporative contribution. Sink region outlined in red. Note, y-axis ranges in b) and c) span a larger array of values since this region received more precipitation than the Front Range.

665



670 Figure B2: (a), (b), (c) Spatial and monthly variation of eastern Plains (EPL) moisture sources averaged from 2000-2022. (a) Map of average tracked evaporation accumulating from May through July. (b) Average monthly regional contributions to the EPL in volume of water vapor ( $m^3$ ). (c) Average cumulative regional contribution across May, June and July to FTR precipitation in volume of water vapor ( $m^3$ ). Note, y-axis ranges in b) and c) span a larger array of values since this region received more precipitation than the Front Range.



675

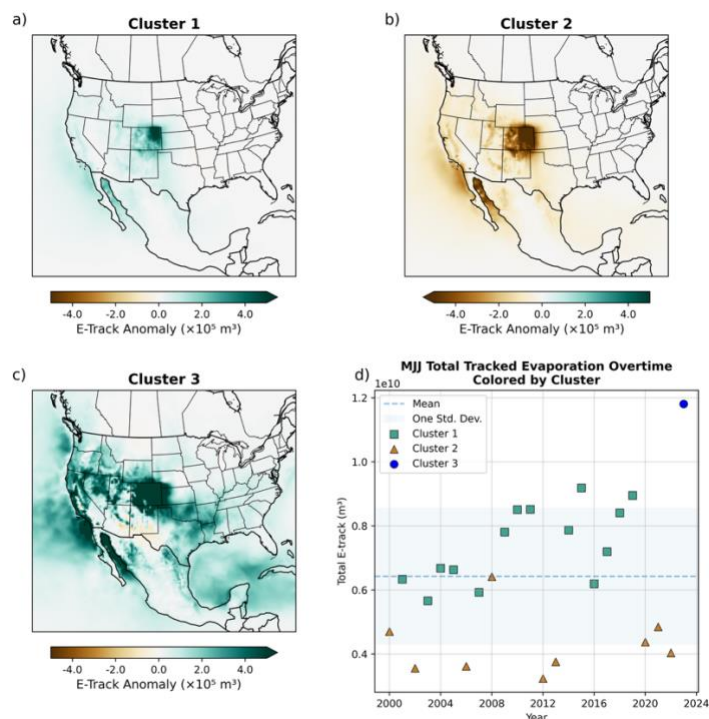


**Figure B3: Spatiotemporal patterns of MJJ evaporation anomalies of eastern Plains (EPL) precipitation from k-means Clustering. (a), (b), (c) Cluster average MJJ moisture contribution. (d) MJJ total precipitation (spatially summed e-track) overtime. Color and shape assigned by cluster number.**

680

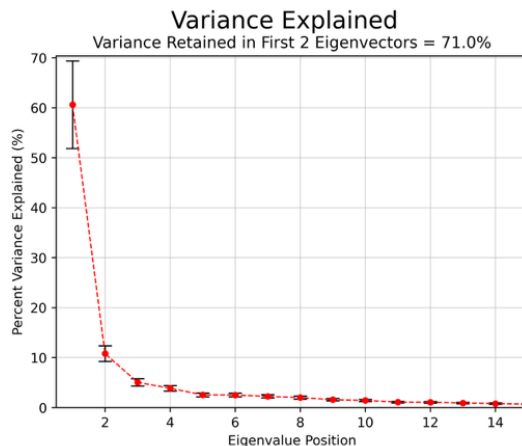
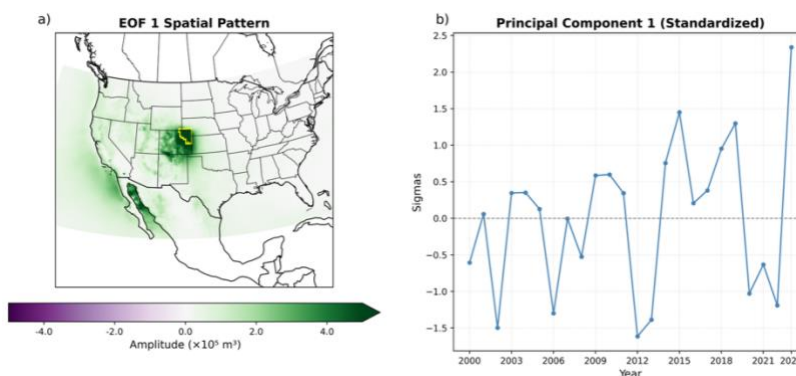


**Figure B4: Results from EOF analysis on the eastern Plains region (EPL). Percent variance explained (PVE) by eigenvectors ranked from least to greatest eigenvalue. Error bars represent 95% confidence bounds as calculated in North et al. (1982) assuming that each MJJ season is independent of one another.**



685



690

**Figure B5:** (a) Spatial pattern of the first empirical orthogonal function (EOF1) of MJJ tracked evaporation anomalies for the eastern Plains region (EPL) from 2000–2023. (b) Standardized principal component time series (PC1) corresponding to EOF1. Sink region marked in yellow.

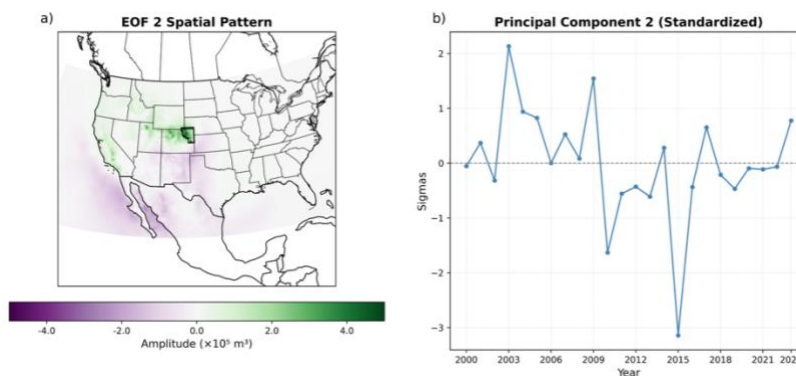
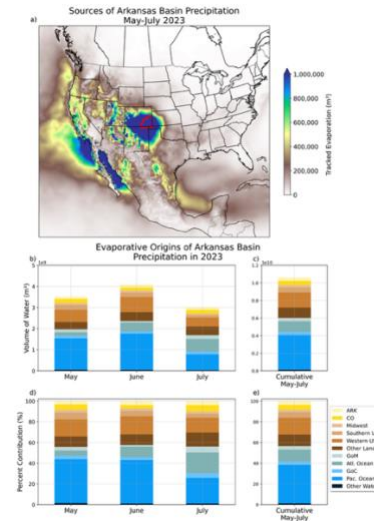


**Figure B6:** (a) Spatial pattern of the second empirical orthogonal function (EOF2) of MJJ tracked evaporation anomalies for the eastern Plains region (EPL) from 2000–2023. (b) Standardized principal component time series (PC2) corresponding to EOF2. Sink region outlined in black.

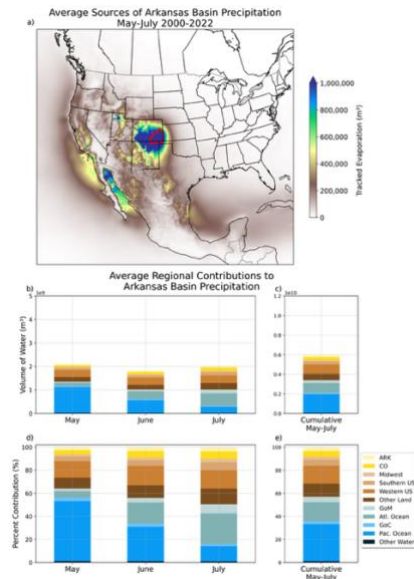


695 **B.2 Arkansas Basin Region Analysis**



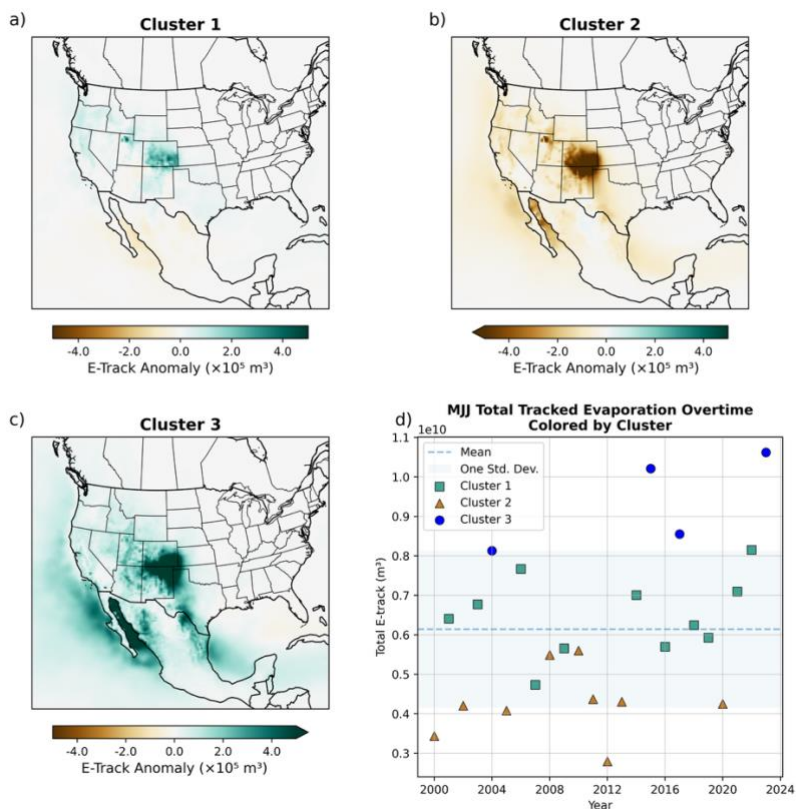
700

**Figure B7:** a), b), c), d), e) Spatial and monthly variation in moisture sources of Arkansas Basin region (ARK) precipitation in May, June, and July of 2023. a) Map of evaporative sources of ARK precipitation accumulating from May through July of 2023. b) Monthly regional contribution to the ARK in volume of water vapor ( $m^3$ ). c) Cumulative regional evaporative contribution across May, June and July of 2023 to ARK precipitation in volume of water vapor ( $m^3$ ). d) Monthly regional evaporative contribution as a percent of total monthly evaporative contribution. e) Cumulative regional contribution as a percent of total monthly evaporative contribution. Sink region outlined in red. Note, y-axis ranges in b) and c) span a larger array of values since this region received more precipitation than the Front Range.



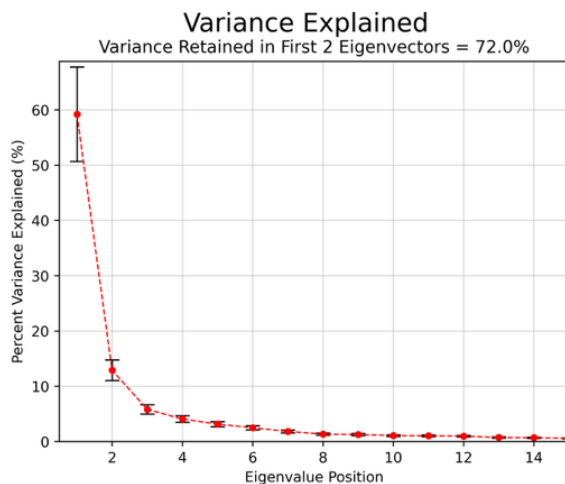
705

**Figure B8:** (a), (b), (c) Spatial and monthly variation of Arkansas Basin (ARK) moisture sources averaged from 2000-2022. (a) Map of average tracked evaporation accumulating from May through July. (b) Average monthly regional contributions to the ARK in volume of water vapor ( $m^3$ ). (c) Average cumulative regional contribution across May, June and July to ARK precipitation in volume of water vapor ( $m^3$ ). Sink region outlined in red. Note, y-axis ranges in b) and c) span a larger array of values since this region received more precipitation than the Front Range.

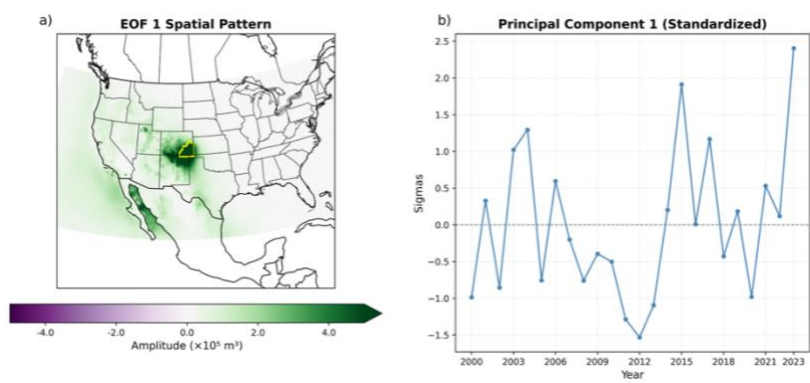


710

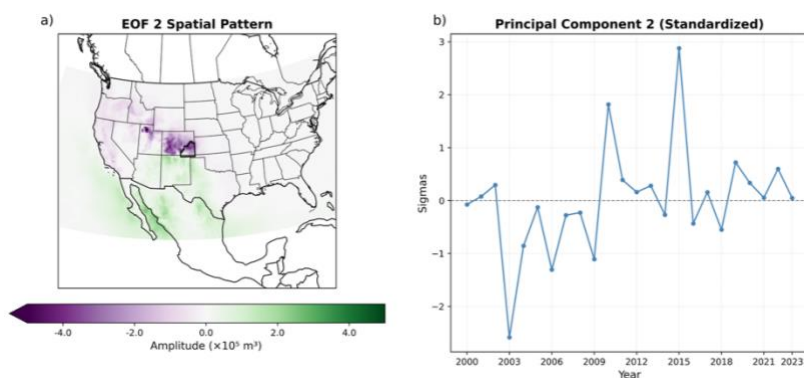
**Figure B9:** Spatiotemporal patterns of MJJ evaporation anomalies of Arkansas Basin (ARK) precipitation from k-means Clustering. (a), (b), (c) Cluster average MJJ moisture contribution. (d) MJJ total precipitation (spatially summed e-track overtime. Color and shape assigned by cluster number.



**715 Figure B10:** Results from EOF analysis on the Arkansas Basin region (ARK). Percent variance explained (PVE) by eigenvectors ranked from least to greatest eigenvalue. Error bars represent 95% confidence bounds as calculated in North et al. (1982) assuming that each MJJ season is independent of one another.

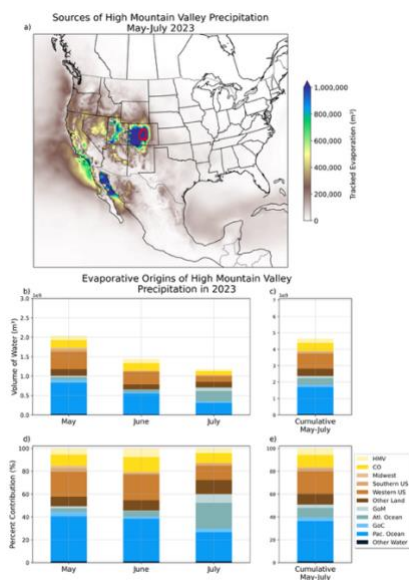


720 **Figure B11:** (a) Spatial pattern of the first empirical orthogonal function (EOF1) of MJJ tracked evaporation anomalies for the Arkansas Basin region (ARK) from 2000–2023. (b) Standardized principal component time series (PC1) corresponding to EOF1. Sink region marked in yellow.



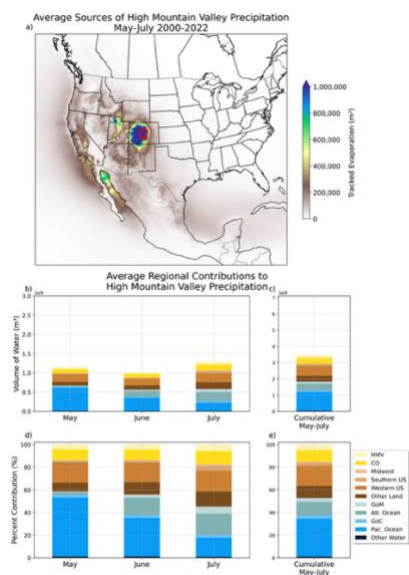
725 **Figure B12:** (a) Spatial pattern of the second empirical orthogonal function (EOF2) of MJJ tracked evaporation anomalies for the Arkansas Basin region (ARK) from 2000–2023. (b) Standardized principal component time series (PC2) corresponding to EOF2. Sink region outlined in black.

### B.3 High Mountain Valley Region Analysis



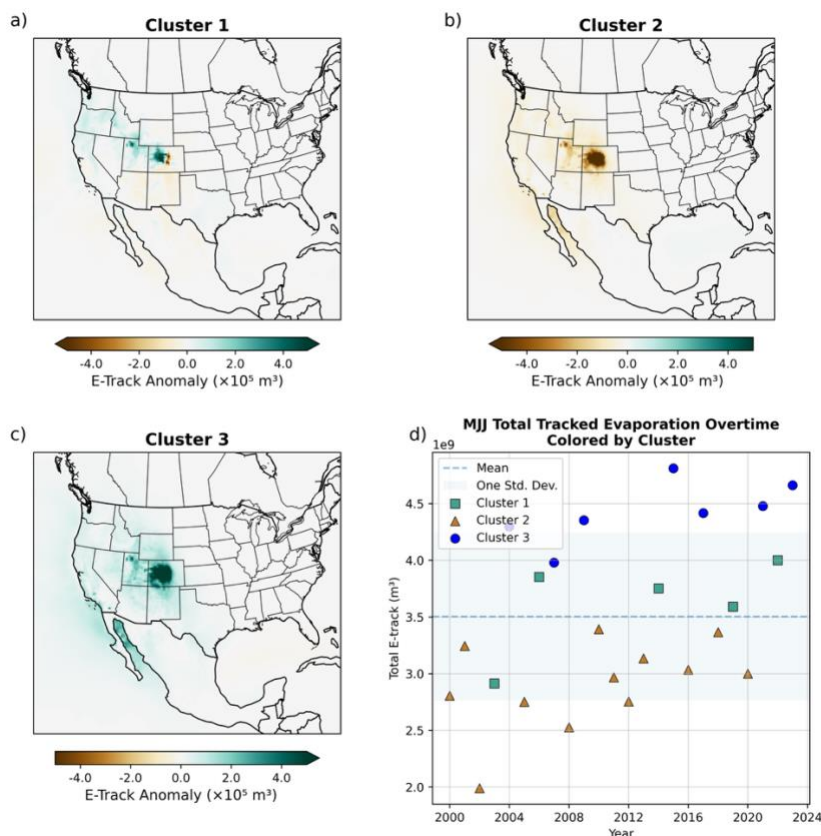
730

**Figure B13:** a), b), c), d), e) Spatial and monthly variation in moisture sources of High Mountain Valley region (HMV) precipitation in May, June, and July of 2023. a) Map of evaporative sources of HMV precipitation accumulating from May through July of 2023. b) Monthly regional contribution to the HMV in volume of water vapor ( $m^3$ ). c) Cumulative regional evaporative contribution across May, June and July of 2023 to HMV precipitation in volume of water vapor ( $m^3$ ). d) Monthly regional evaporative contribution as a percent of total monthly evaporative contribution. e) Cumulative regional contribution as a percent of total monthly evaporative contribution. Sink region outlined in red.

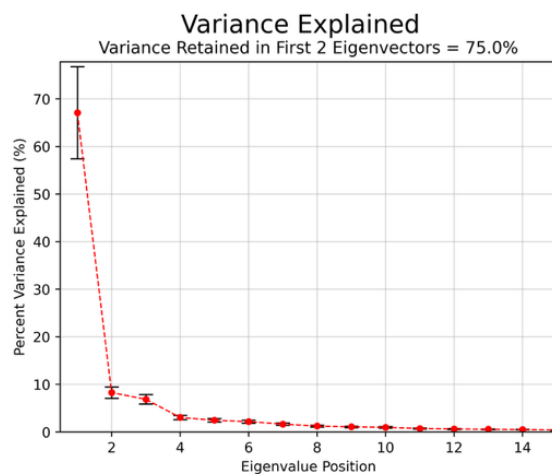


735

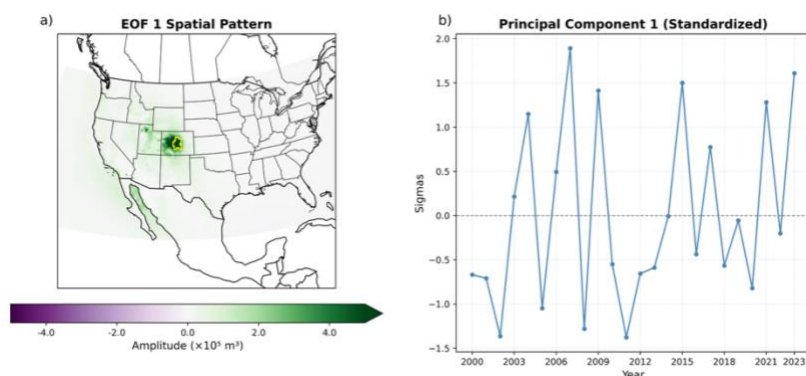
**Figure B14:** (a), (b), (c) Spatial and monthly variation of High Mountain Valley (HMV) moisture sources averaged from 2000-2022. (a) Map of average tracked evaporation accumulating from May through July. (b) Average monthly regional contributions to the HMV in volume of water vapor ( $m^3$ ). (c) Average cumulative regional contribution across May, June and July to HMV precipitation in volume of water vapor ( $m^3$ ). Sink region outlined in red.



740 **Figure B15: Spatiotemporal patterns of MJJ evaporation anomalies of High Mountain Valley (HMV) precipitation from k-means Clustering. (a), (b), (c) Cluster average MJJ moisture contribution. (d) MJJ total precipitation (spatially summed e-track) overtime. Color and shape assigned by cluster number.**



745 **Figure B16: Results from EOF analysis on the High Mountain Valley region (HMV). Percent variance explained (PVE) by eigenvectors ranked from least to greatest eigenvalue. Error bars represent 95% confidence bounds as calculated in North et al. (1982) assuming that each MJJ season is independent of one another.**



750 **Figure B17: (a) Spatial pattern of the first empirical orthogonal function (EOF1) of MJJ tracked evaporation anomalies for the High Mountain Valley region (HMV) from 2000–2023. (b) Standardized principal component time series (PC1) corresponding to EOF1. Sink region marked in yellow.**

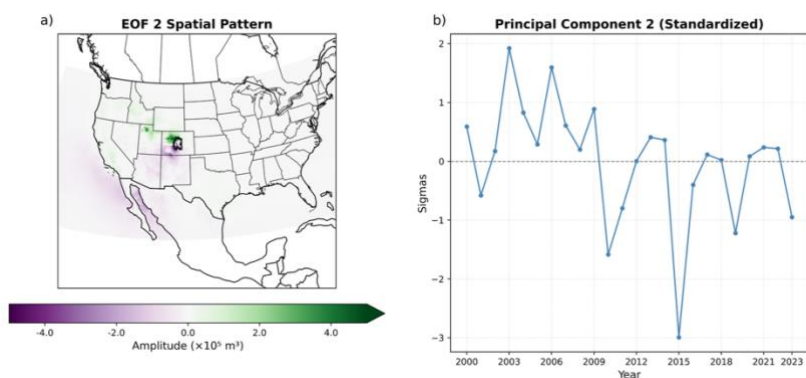
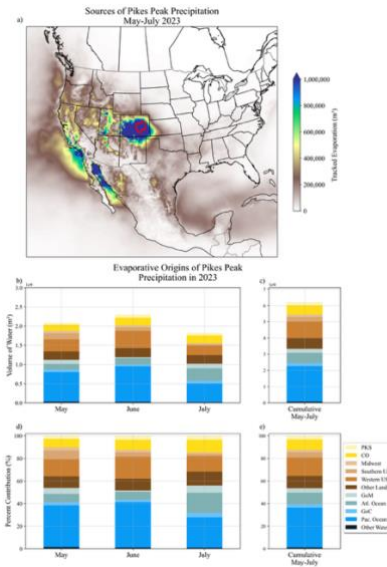


**Figure B18: (a) Spatial pattern of the second empirical orthogonal function (EOF2) of MJJ tracked evaporation anomalies for the High Mountain Valley region (HMV) from 2000–2023. (b) Standardized principal component time series (PC2) corresponding to EOF2. Sink region outlined in black.**

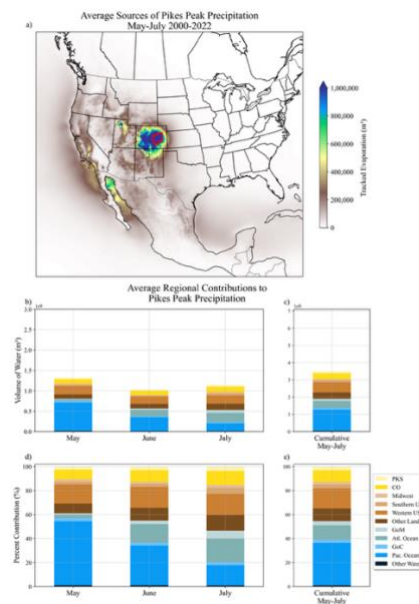


755 **B.4 Pikes Peak Region Analysis**



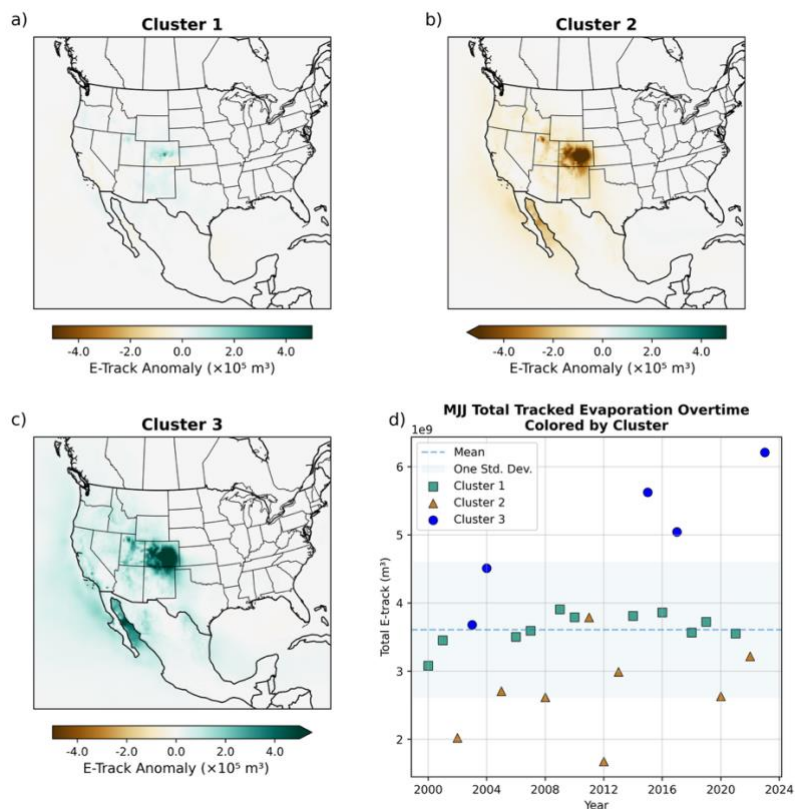
760

**Figure B19:** a), b), c), d), e) Spatial and monthly variation in moisture sources of Pikes Peak region (PKS) precipitation in May, June, and July of 2023. a) Map of evaporative sources of PKS precipitation accumulating from May through July of 2023. b) Monthly regional contribution to the PKS in volume of water vapor ( $m^3$ ). c) Cumulative regional evaporative contribution across May, June and July of 2023 to PKS precipitation in volume of water vapor ( $m^3$ ). d) Monthly regional evaporative contribution as a percent of total monthly evaporative contribution. e) Cumulative regional contribution as a percent of total monthly evaporative contribution. Sink region outlined in red.

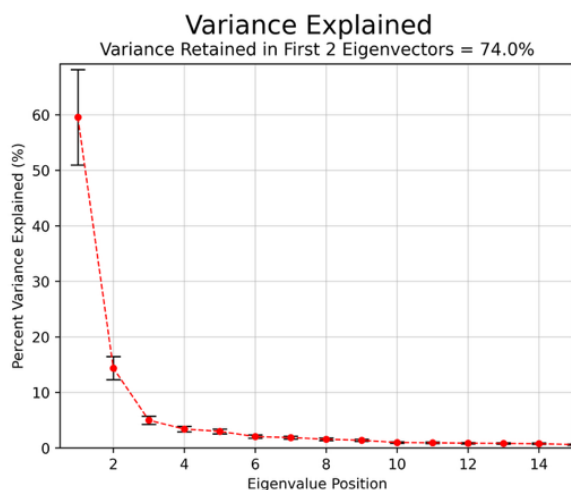


765

**Figure B20:** (a), (b), (c) Spatial and monthly variation of Pikes Peak (PKS) moisture sources averaged from 2000-2022. (a) Map of average tracked evaporation accumulating from May through July. (b) Average monthly regional contributions to the PKS in volume of water vapor ( $m^3$ ). (c) Average cumulative regional contribution across May, June and July to PKS precipitation in volume of water vapor ( $m^3$ ). Sink region outlined in red.



770 **Figure B21: Spatiotemporal patterns of MJJ evaporation anomalies of Pikes Peak (PKS) precipitation from k-means Clustering. (a), (b), (c) Cluster average MJJ moisture contribution. (d) MJJ total precipitation (spatially summed e-track) overtime. Color and shape assigned by cluster number.**



775 **Figure B22: Results from EOF analysis on the Pikes Peak region (PKS). Percent variance explained (PVE) by eigenvectors ranked from least to greatest eigenvalue. Error bars represent 95% confidence bounds as calculated in North et al. (1982) assuming that each MJJ season is independent of one another.**

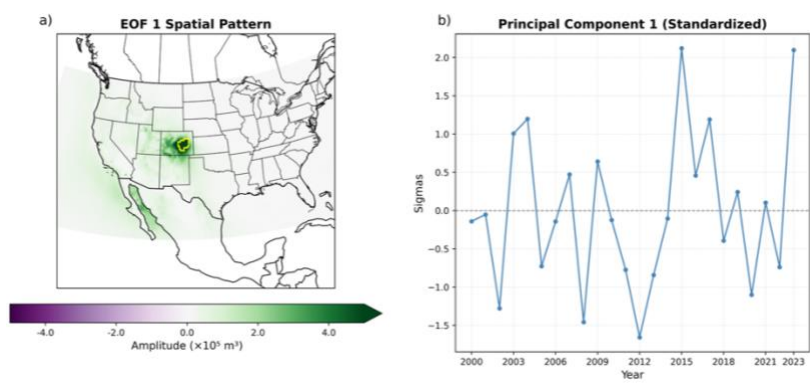


Figure B23: (a) Spatial pattern of the first empirical orthogonal function (EOF1) of MJJ tracked evaporation anomalies for the Pikes Peak region (PKS) from 2000–2023. (b) Standardized principal component time series (PC1) corresponding to EOF1. Sink region marked in yellow.

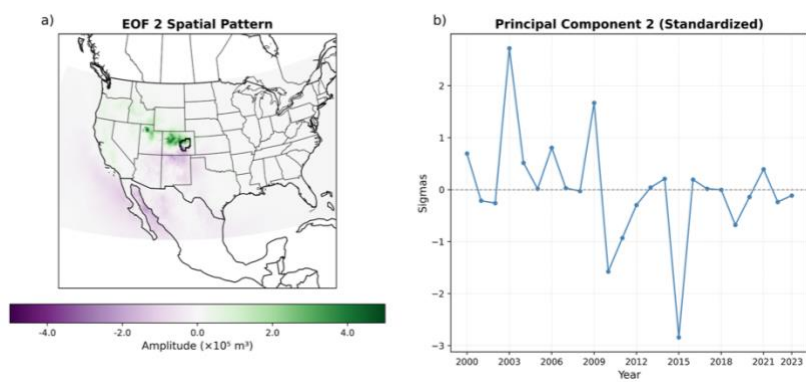


Figure B24: (a) Spatial pattern of the second empirical orthogonal function (EOF2) of MJJ tracked evaporation anomalies for the Pikes Peak region (PKS) from 2000–2023. (b) Standardized principal component time series (PC2) corresponding to EOF2. Sink region outlined in black.

### Code availability

785 The code used to plot original figures and analyze moisture source data for this manuscript can be found on GitHub (Humphreys, 2026).

### Data availability

790 Monthly moisture source outputs from the Water Accounting Model 2 Layers (WAM2layers) model, as well as corresponding region masks, are available from the associated Dryad archive (Humphreys et al., 2026). The underlying ERA5 data used to run the WAM2layers model are publicly available through ECMWF at <https://cds.climate.copernicus.eu/datasets/reanalysis-era5-single-levels?tab=download> for surface variables (total precipitation, evaporation, surface pressure, and total column water) and [https://cds.climate.copernicus.eu/datasets/reanalysis-era5-complete?tab=d\\_download](https://cds.climate.copernicus.eu/datasets/reanalysis-era5-complete?tab=d_download) for model-level, 3d variables



795 (u and v components of the wind and specific humidity). The Parameter-elevation Regressions on Independent Slopes Model (PRISM) gridded monthly precipitation data are supplied by Oregon State University and can be downloaded at <https://prism.oregonstate.edu/downloads/>.

### **Author contributions**

K.H. led this study, including conceptualization, data curation, formal analysis, investigation, methodology, project administration, visualization, and writing. P.K. and R.S. contributed to funding, conceptualization, investigation, and writing. P.G. And J.E. contributed to investigation and writing.

### 800 **Competing interests**

The authors declare that they have no conflict of interest.

### **Disclaimer**

805 Publisher's note: Copernicus Publications remains neutral regarding jurisdictional claims made in the text, published maps, institutional affiliations, or any other geographical representation in this paper. While Copernicus Publications makes every effort to include appropriate place names, the final responsibility lies with the authors. Views expressed in the text are those of the authors and do not necessarily reflect the views of the publisher.

### **Acknowledgements**

The authors would like to acknowledge Kevin Houck, the emergency management lead for the Colorado Water Conservation Board. Kevin was integral in both funding and motivating this research.

### 810 **Financial support**

We would like to acknowledge the Colorado Water Conservation Board for providing the funds to complete this publication.



## References

- Arias, P. A., Martínez, J. A., and Vieira, S. C.: Moisture sources to the 2010–2012 anomalous wet season in northern South America, *Clim Dyn*, 45, 2861–2884, <https://doi.org/10.1007/s00382-015-2511-7>, 2015.
- 815 Beck, H. E., Pan, M., Roy, T., Weedon, G. P., Pappenberger, F., Van Dijk, A. I. J. M., Huffman, G. J., Adler, R. F., and Wood, E. F.: Daily evaluation of 26 precipitation datasets using Stage-IV gauge-radar data for the CONUS, *Hydrol. Earth Syst. Sci.*, 23, 207–224, <https://doi.org/10.5194/hess-23-207-2019>, 2019.
- Bosilovich, M. G. and Schubert, S. D.: Water Vapor Tracers as Diagnostics of the Regional Hydrologic Cycle, *J. Hydrometeorol.*, 3, 149–165, [https://doi.org/10.1175/1525-7541\(2002\)003<0149:WVTADO>2.0.CO;2](https://doi.org/10.1175/1525-7541(2002)003<0149:WVTADO>2.0.CO;2), 2002.
- 820 Brubaker, K. L., Entekhabi, D., and Eagleson, P. S.: Estimation of Continental Precipitation Recycling, *J. Climate*, 6, 1077–1089, [https://doi.org/10.1175/1520-0442\(1993\)006<1077:EOCPR>2.0.CO;2](https://doi.org/10.1175/1520-0442(1993)006<1077:EOCPR>2.0.CO;2), 1993.
- Brubaker, K. L., Dirmeyer, P. A., Sudradjat, A., Levy, B. S., and Bernal, F.: A 36-yr Climatological Description of the Evaporative Sources of Warm-Season Precipitation in the Mississippi River Basin, *J. Hydrometeorol.*, 2, 537–557, [https://doi.org/10.1175/1525-7541\(2001\)002<0537:AYCDOT>2.0.CO;2](https://doi.org/10.1175/1525-7541(2001)002<0537:AYCDOT>2.0.CO;2), 2001.
- 825 Burde, G. I. and Zangvil, A.: The Estimation of Regional Precipitation Recycling. Part I: Review of Recycling Models, *J. Climate*, 14, 2497–2508, [https://doi.org/10.1175/1520-0442\(2001\)014<2497:TEORPR>2.0.CO;2](https://doi.org/10.1175/1520-0442(2001)014<2497:TEORPR>2.0.CO;2), 2001.
- Ciric, D., Nieto, R., Losada, L., Drumond, A., and Gimeno, L.: The Mediterranean Moisture Contribution to Climatological and Extreme Monthly Continental Precipitation, *Water*, 10, 519, <https://doi.org/10.3390/w10040519>, 2018.
- 830 Cloux, S., Garaboa-Paz, D., Insua-Costa, D., Miguez-Macho, G., and Pérez-Muñuzuri, V.: Extreme precipitation events in the Mediterranean area: contrasting two different models for moisture source identification, *Hydrol. Earth Syst. Sci.*, 25, 6465–6477, <https://doi.org/10.5194/hess-25-6465-2021>, 2021.
- Colorado Climate Center: Climate at a Glance Rank Maps, [https://climate.colostate.edu/co\\_cag/rank\\_maps.html](https://climate.colostate.edu/co_cag/rank_maps.html) (last access April 30, 2025), 2024.
- 835 Crossett, C. C., Betts, A. K., Dupigny-Giroux, L.-A. L., and Bombles, A.: Evaluation of Daily Precipitation from the ERA5 Global Reanalysis against GHCN Observations in the Northeastern United States, *Climate*, 8, 148, <https://doi.org/10.3390/cli8120148>, 2020.
- Daly, C., Doggett, M. K., Smith, J. I., Olson, K. V., Halbleib, M. D., Dimcovic, Z., Keon, D., Loiselle, R. A., Steinberg, B., Ryan, A. D., Pancake, C. M., and Kaspar, E. M.: Challenges in Observation-Based Mapping of Daily Precipitation across the Conterminous United States, *Journal of Atmospheric and Oceanic Technology*, 38, 1979–1992, <https://doi.org/10.1175/JTECH-D-21-0054.1>, 2021.
- 840 Dansgaard, W.: Stable isotopes in precipitation, *Tellus A: Dynamic Meteorology and Oceanography*, 16, 436, <https://doi.org/10.3402/tellusa.v16i4.8993>, 1964.



- Doesken, N. J., Sr., R. A. P., and Bliss, O. A. P.: Climate of Colorado, Colorado Climate Center and Colorado State University, 845 <https://hdl.handle.net/10217/236290>, 2003.
- Dirmeyer, P. A. and Brubaker, K. L.: Contrasting evaporative moisture sources during the drought of 1988 and the flood of 1993, *J. Geophys. Res.*, 104, 19383–19397, <https://doi.org/10.1029/1999JD900222>, 1999.
- Dirmeyer, P. A., Brubaker, K. L., and DelSole, T.: Import and export of atmospheric water vapor between nations, *Journal of Hydrology*, 365, 11–22, <https://doi.org/10.1016/j.jhydrol.2008.11.016>, 2009.
- 850 Drumond, A., Nieto, R., Hernandez, E., and Gimeno, L.: A Lagrangian analysis of the variation in moisture sources related to drier and wetter conditions in regions around the Mediterranean Basin, *Nat. Hazards Earth Syst. Sci.*, 11, 2307–2320, <https://doi.org/10.5194/nhess-11-2307-2011>, 2011.
- Eden, J. M., Wolter, K., Otto, F. E. L., and Jan Van Oldenborgh, G.: Multi-method attribution analysis of extreme precipitation in Boulder, Colorado, *Environ. Res. Lett.*, 11, 124009, <https://doi.org/10.1088/1748-9326/11/12/124009>, 2016.
- 855 Erlingis, J. M., Gourley, J. J., and Basara, J. B.: Diagnosing Moisture Sources for Flash Floods in the United States. Part I: Kinematic Trajectories, *Journal of Hydrometeorology*, 20, 1495–1509, <https://doi.org/10.1175/JHM-D-18-0119.1>, 2019a.
- Erlingis, J. M., Gourley, J. J., and Basara, J. B.: Diagnosing Moisture Sources for Flash Floods in the United States. Part II: Terrestrial and Oceanic Sources of Moisture, *Journal of Hydrometeorology*, 20, 1511–1531, <https://doi.org/10.1175/JHM-D-18-0120.1>, 2019b.
- 860 Flanders Marine Institute (VLIZ), Belgium: IHO Sea Areas, version 3, Marine Data Archive [data set] <https://doi.org/10.14284/323>, 2018.
- Flanders Marine Institute (VLIZ), Belgium: Global Oceans and Seas, version 1, Marine Data Archive [data set] <https://doi.org/10.14284/542>, 2021.
- Gimeno, L., Vázquez, M., Eiras-Barca, J., Sorí, R., Stojanovic, M., Algarra, I., Nieto, R., Ramos, A. M., Durán-Quesada, A. 865 M., and Dominguez, F.: Recent progress on the sources of continental precipitation as revealed by moisture transport analysis, *Earth-Science Reviews*, 201, 103070, <https://doi.org/10.1016/j.earscirev.2019.103070>, 2020.
- Gimeno, L., Eiras-Barca, J., Durán-Quesada, A. M., Dominguez, F., Van Der Ent, R., Sodemann, H., Sánchez-Murillo, R., Nieto, R., and Kirchner, J. W.: The residence time of water vapour in the atmosphere, *Nat Rev Earth Environ*, 2, 558–569, <https://doi.org/10.1038/s43017-021-00181-9>, 2021.
- 870 Gustafsson, M., Rayner, D., and Chen, D.: Extreme rainfall events in southern Sweden: where does the moisture come from?, *Tellus A: Dynamic Meteorology and Oceanography*, 62, 605, <https://doi.org/10.1111/j.1600-0870.2010.00456.x>, 2010.
- Hersbach, H., Bell, B., Berrisford, P., Hirahara, S., Horányi, A., Muñoz-Sabater, J., Nicolas, J., Peubey, C., Radu, R., Schepers, D., Simmons, A., Soci, C., Abdalla, S., Abellan, X., Balsamo, G., Bechtold, P., Biavati, G., Bidlot, J., Bonavita, M., De Chiara, G., Dahlgren, P., Dee, D., Diamantakis, M., Dragani, R., Flemming, J., Forbes, R., Fuentes, M., Geer, A., Haimberger, L., 875 Healy, S., Hogan, R. J., Hólm, E., Janisková, M., Keeley, S., Laloyaux, P., Lopez, P., Lupu, C., Radnoti, G., De Rosnay, P., Rozum, I., Vamborg, F., Villaume, S., and Thépaut, J.: The ERA5 global reanalysis, *Quart J Royal Meteorol Soc*, 146, 1999–2049, <https://doi.org/10.1002/qj.3803>, 2020 (last access: February 2026).



- Hu, H. and Dominguez, F.: Evaluation of Oceanic and Terrestrial Sources of Moisture for the North American Monsoon Using Numerical Models and Precipitation Stable Isotopes, *Journal of Hydrometeorology*, 16, 19–35, <https://doi.org/10.1175/JHM-D-14-0073.1>, 2015.
- 880 Humphreys, K. V.: *Eastern\_Colorado\_Moisture\_Sources\_Analysis*, GitHub [code], (DOI will be provided for final publication), 2026.
- Humphreys, K. V., Keys, P. W., Schumacher, R. S., Escobedo, J., and Gobel, P.: Local moisture recycling across the globe, *Dryad* [data set], (DOI will be provided for final publication), 2026.
- 885 Insua-Costa, D. and Miguez-Macho, G.: A new moisture tagging capability in the Weather Research and Forecasting model: formulation, validation and application to the 2014 Great Lake-effect snowstorm, *Earth Syst. Dynam.*, 9, 167–185, <https://doi.org/10.5194/esd-9-167-2018>, 2018.
- Jana, S., Rajagopalan, B., Alexander, M. A., and Ray, A. J.: Understanding the Dominant Sources and Tracks of Moisture for Summer Rainfall in the Southwest United States, *JGR Atmospheres*, 123, 4850–4870, <https://doi.org/10.1029/2017JD027652>,  
890 2018.
- Kalverla, P., Benedict, I., Weijenborg, C., and Van Der Ent, R. J.: Atmospheric moisture tracking with WAM2layers v3, *Geosci. Model Dev.*, 18, 4335–4352, <https://doi.org/10.5194/gmd-18-4335-2025>, 2025.
- Keys, P. W., Van Der Ent, R. J., Gordon, L. J., Hoff, H., Nikoli, R., and Savenije, H. H. G.: Analyzing precipitationsheds to understand the vulnerability of rainfall dependent regions, *Biogeosciences*, 9, 733–746, [https://doi.org/10.5194/bg-9-733-](https://doi.org/10.5194/bg-9-733-2012)  
895 [2012](https://doi.org/10.5194/bg-9-733-2012), 2012.
- Keys, P. W., Barnes, E. A., Van Der Ent, R. J., and Gordon, L. J.: Variability of moisture recycling using a precipitationshed framework, *Hydrol. Earth Syst. Sci.*, 18, 3937–3950, <https://doi.org/10.5194/hess-18-3937-2014>, 2014.
- Kim, S. and Dominguez, F.: Warm Season Extreme Flood Events in the Midwestern US—Sources of Moisture and Physical Mechanisms, *JGR Atmospheres*, 128, e2022JD038208, <https://doi.org/10.1029/2022JD038208>, 2023.
- 900 Koster, R. D., Dirmeyer, P. A., Guo, Z., Bonan, G., Chan, E., Cox, P., Gordon, C. T., Kanae, S., Kowalczyk, E., Lawrence, D., Liu, P., Lu, C.-H., Malyshev, S., McAvaney, B., Mitchell, K., Mocko, D., Oki, T., Oleson, K., Pitman, A., Sud, Y. C., Taylor, C. M., Verseghy, D., Vasic, R., Xue, Y., and Yamada, T.: Regions of Strong Coupling Between Soil Moisture and Precipitation, *Science*, 305, 1138–1140, <https://doi.org/10.1126/science.1100217>, 2004.
- Knoche, H. R. and Kunstmann, H.: Tracking atmospheric water pathways by direct evaporation tagging: A case study for West  
905 Africa, *JGR Atmospheres*, 118, <https://doi.org/10.1002/2013JD019976>, 2013.
- Liu, X., Guo, C., Zhang, J., Liu, Y., Xiao, M., Wu, Y., Li, B., and Zhao, T.: Moisture sources of precipitation over the Pearl River Basin in South China, *Intl Journal of Climatology*, 44, 2160–2173, <https://doi.org/10.1002/joc.8447>, 2024.
- Liu, Y., Zhang, C., Tang, Q., Hosseini-Moghari, S.-M., Haile, G. G., Li, L., Li, W., Yang, K., Van Der Ent, R. J., and Chen, D.: Moisture source variations for summer rainfall in different intensity classes over Huaihe River Valley, China, *Clim Dyn*,  
910 57, 1121–1133, <https://doi.org/10.1007/s00382-021-05762-4>, 2021.



- Lloyd, S.: Least squares quantization in PCM, *IEEE Trans. Inform. Theory*, 28, 129–137, <https://doi.org/10.1109/TIT.1982.1056489>, 1982.
- Marengo, J. A., Alves, L. M., Soares, W. R., Rodriguez, D. A., Camargo, H., Riveros, M. P., and Pabló, A. D.: Two Contrasting Severe Seasonal Extremes in Tropical South America in 2012: Flood in Amazonia and Drought in Northeast Brazil, *Journal of Climate*, 26, 9137–9154, <https://doi.org/10.1175/JCLI-D-12-00642.1>, 2013.
- 915 McKee, T., Doesken, N. J., Kliest, J., Shrier, C. J., and Stanton, W. P.: A History of Drought in Colorado: Lessons Learned and What Lies Ahead, Colorado State University and Colorado Water Resources Research Institute, 2000.
- North, G. R., Bell, T. L., Cahalan, R. F., and Moeng, F. J.: Sampling Errors in the Estimation of Empirical Orthogonal Functions, *Mon. Wea. Rev.*, 110, 699–706, [https://doi.org/10.1175/1520-0493\(1982\)110<0699:SEITEO>2.0.CO;2](https://doi.org/10.1175/1520-0493(1982)110<0699:SEITEO>2.0.CO;2), 1982.
- 920 Pedregosa, F., Varoquaux, G., Gramfort, A., Michel, V., Thirion, B., Grisel, O., Blondel, M., Müller, A., Nothman, J., Louppe, G., Prettenhofer, P., Weiss, R., Dubourg, V., Vanderplas, J., Passos, A., Cournapeau, D., Brucher, M., Perrot, M., and Duchesnay, É.: Scikit-learn: Machine Learning in Python, <https://doi.org/10.48550/ARXIV.1201.0490>, 2012.
- Pinto, J. G., Ulbrich, S., Parodi, A., Rudari, R., Boni, G., and Ulbrich, U.: Identification and ranking of extraordinary rainfall events over Northwest Italy: The role of Atlantic moisture, *JGR Atmospheres*, 118, 2085–2097, <https://doi.org/10.1002/jgrd.50179>, 2013.
- 925 Rapolaki, R. S., Blamey, R. C., Hermes, J. C., and Reason, C. J. C.: Moisture sources and transport during an extreme rainfall event over the Limpopo River Basin, southern Africa, *Atmospheric Research*, 264, 105849, <https://doi.org/10.1016/j.atmosres.2021.105849>, 2021.
- Rios-Entenza, A. and Miguez-Macho, G.: Moisture recycling and the maximum of precipitation in spring in the Iberian Peninsula, *Clim Dyn*, 42, 3207–3231, <https://doi.org/10.1007/s00382-013-1971-x>, 2014.
- Schumacher, R., Bolinger, R., and Lukas, J.: Development of Alternate Climate Divisions for Colorado Based on Gridded Data, *JoASC*, 2024, 1–9, <https://doi.org/10.46275/JOASC.2024.06.002>, 2024.
- Skinner, C. B., Harrington, T. S., Barlow, M., and Agel, L.: The contribution of precipitation recycling to North American wet and dry precipitation extremes, *Environ. Res.: Climate*, 2, 045010, <https://doi.org/10.1088/2752-5295/acffea>, 2023.
- 935 Sprenger, M., Leistert, H., Gimbel, K., and Weiler, M.: Illuminating hydrological processes at the soil-vegetation-atmosphere interface with water stable isotopes, *Reviews of Geophysics*, 54, 674–704, <https://doi.org/10.1002/2015RG000515>, 2016.
- Syakur, M. A., Khotimah, B. K., Rochman, E. M. S., and Satoto, B. D.: Integration K-Means Clustering Method and Elbow Method for Identification of The Best Customer Profile Cluster, *IOP Conf. Ser.: Mater. Sci. Eng.*, 336, 012017, <https://doi.org/10.1088/1757-899X/336/1/012017>, 2018.
- 940 Tarek, M., Brissette, F. P., and Arsenault, R.: Evaluation of the ERA5 reanalysis as a potential reference dataset for hydrological modelling over North America, *Hydrol. Earth Syst. Sci.*, 24, 2527–2544, <https://doi.org/10.5194/hess-24-2527-2020>, 2020.
- Tuinenburg, O. A. and Staal, A.: Tracking the global flows of atmospheric moisture and associated uncertainties, *Hydrol. Earth Syst. Sci.*, 24, 2419–2435, <https://doi.org/10.5194/hess-24-2419-2020>, 2020.



- 945 Tuinenburg, O. A., Hutjes, R. W. A., and Kabat, P.: The fate of evaporated water from the Ganges basin, *J. Geophys. Res.*, 117, 2011JD016221, <https://doi.org/10.1029/2011JD016221>, 2012.
- U.S. Census Bureau: RACE, [https://data.census.gov/table/DECENNIALPL2020.P1?g=040XX00US08\\$0500000&tp=true](https://data.census.gov/table/DECENNIALPL2020.P1?g=040XX00US08$0500000&tp=true) (last access: 16 February 2026), 2020.
- van der Ent, R. J. and Tuinenburg, O. A.: The residence time of water in the atmosphere revisited, *Hydrol. Earth Syst. Sci.*, 950 21, 779–790, <https://doi.org/10.5194/hess-21-779-2017>, 2017.
- van der Ent, R. J., Savenije, H. H. G., Schaeffli, B., and Steele-Dunne, S. C.: Origin and fate of atmospheric moisture over continents, *Water Resources Research*, 46, 2010WR009127, <https://doi.org/10.1029/2010WR009127>, 2010.
- van Der Ent, R. J., Tuinenburg, O. A., Knoche, H.-R., Kunstmann, H., and Savenije, H. H. G.: Should we use a simple or complex model for moisture recycling and atmospheric moisture tracking?, *Hydrol. Earth Syst. Sci.*, 17, 4869–4884, 955 <https://doi.org/10.5194/hess-17-4869-2013>, 2013.
- van der Ent, R. J., Wang-Erlandsson, L., Keys, P. W., and Savenije, H. H. G.: Contrasting roles of interception and transpiration in the hydrological cycle – Part 2: Moisture recycling, *Earth Syst. Dynam.*, 5, 471–489, <https://doi.org/10.5194/esd-5-471-2014>, 2014.
- van der Ent, R. J., Benedict, I. B., Weijenberg, C., Cömert, T., van de Koppel, N., Guo, L., de Feiter, V., and Kalverla, P.: 960 WAM2layers, Zenodo [code], <https://doi.org/10.5281/ZENODO.8172344>, 2023.
- Wei, J., Dirmeyer, P. A., Wisser, D., Bosilovich, M. G., and Mocko, D. M.: Where Does the Irrigation Water Go? An Estimate of the Contribution of Irrigation to Precipitation Using MERRA, *Journal of Hydrometeorology*, 14, 275–289, <https://doi.org/10.1175/JHM-D-12-079.1>, 2013.
- Yang, Z., Qian, Y., Xue, P., Wang, J., Chakraborty, T. C., Pringle, W. J., Li, J., and Chen, X.: Moisture Sources of Precipitation 965 in the Great Lakes Region: Climatology and Recent Changes, *Geophysical Research Letters*, 50, e2022GL100682, <https://doi.org/10.1029/2022GL100682>, 2023.
- Zhang, C., Tang, Q., Zhao, Y., Chen, D., Huang, J., Liu, Y., and Zhang, X.: Moisture Source Differences Between the 2020 and 1998 Super Meiyu-Flood Events in the Yangtze River Valley, *Weather and Climate Extremes*, 43, 100644, <https://doi.org/10.1016/j.wace.2024.100644>, 2024.
- 970 Zhang, X., Liu, Z., Liu, Y., Jiang, L., Wang, R., Jiang, H., Li, J., Tang, Q., and Yao, Z.: Examining moisture contribution for precipitation in response to climate change and anthropogenic factors in Hengduan Mountain Region, China, *Journal of Hydrology*, 620, 129562, <https://doi.org/10.1016/j.jhydrol.2023.129562>, 2023.
- Zhao, Y., Xu, X., Zhao, T., Xu, H., Mao, F., Sun, H., and Wang, Y.: Extreme precipitation events in East China and associated moisture transport pathways, *Sci. China Earth Sci.*, 59, 1854–1872, <https://doi.org/10.1007/s11430-016-5315-7>, 2016.
- 975 Zhuang, J., Dussin, Raphael, Huard, D., Bourgault, P., Banihirwe, A., Raynaud, S., Malevich, B., Schupfner, M., Gauthier, C., Levang, S., Jüling, A., Almansi, M., RichardScottOZ, RondeauG, Rasp, S., Smith, T. J., Mares, B., Stachelek, J., Plough, M., Pierre, Bell, R., Caneill, R., and Li, X.: pangeo-data/xESMF: v0.8.10, Zenodo [code] , <https://doi.org/10.5281/ZENODO.4294774>, 2025.